Laboratory simulated acid-sulfate weathering of basaltic materials: Implications for formation of sulfates at Meridiani Planum and Gusev Crater, Mars

D. C. Golden[a], Douglas W. Ming[b], Richard V. Morris[b], and Stanley A. Mertzman[c]

[a]ESCG/UTC-HS, Mail Code JE 23, 2224 Bay Area Blvd., Box 7, Houston, Texas 77058

[b]Astromaterials Research and Exploration Science Directorate,
NASA Johnson Space Center, Houston, Texas 77058

[c]Franklin and Marshall College, Lancaster, PA 17604

Journal of Geophysical Research – Planets
In Press

Laboratory simulated acid-sulfate weathering of basaltic materials: Implications for formation of sulfates at Meridiani Planum and Gusev Crater, Mars

D. C. Golden[a], Douglas W. Ming[b,*], Richard V. Morris[b], and Stanley A. Mertzman[c]

[a]ESCG/UTC-HS, Mail Code JE 23, 2224 Bay Area Blvd., Box 7, Houston, Texas 77058

[b]Astromaterials Research and Exploration Science Directorate,
NASA Johnson Space Center, Houston, Texas 77058

[c]Franklin and Marshall College, Lancaster, PA 17604

*Corresponding author: *E-mail address:* douglas.w.ming@nasa.gov

Abstract

Acid-sulfate weathering of basaltic materials is a candidate formation process for the sulfate-rich outcrops and rocks at the MER rover *Opportunity* and *Spirit* landing sites. To determine the style of acid-sulfate weathering on Mars, we weathered basaltic materials (olivine-rich glassy basaltic sand and plagioclase feldspar-rich basaltic tephra) in the laboratory under different oxidative, acid-sulfate conditions and characterized the alteration products. We investigated alteration by (1) sulfuric-acid vapor (acid fog), (2) three-step hydrothermal leaching treatment approximating an "open system" and (3) single-step hydrothermal batch treatment approximating a "closed system." In acid fog experiments, Al, Fe, and Ca sulfates and amorphous silica formed from plagioclase-rich tephra, and Mg and Ca sulfates and amorphous silica formed from the olivine-rich sands. In three-step leaching experiments, only amorphous Si formed from the plagioclase-rich basaltic tephra, and jarosite, Mg and Ca sulfates and amorphous silica formed from olivine-rich basaltic sand. Amorphous silica formed under single-step experiments for both starting materials. Based upon our experiments, jarosite formation in Meridiani outcrop is potential evidence for an open system acid-sulfate weathering regime. Waters rich in sulfuric acid percolated through basaltic sediment, dissolving basaltic phases (e.g., olivine) and forming jarosite, other sulfates, and iron oxides. Aqueous alteration of outcrops and rocks on the West Spur of the Columbia Hills may have occurred when vapors rich in SO_2 from volcanic sources reacted with basaltic materials. Soluble ions from the host rock (e.g., olivine) reacted with S to form Ca-, Mg-, and other sulfates along with iron oxides and oxyhydroxides.

Keywords: Mars, Meridiani Planum, Gusev crater, sulfates, jarosite, acid-sulfate weathering

1. Introduction

The Athena Science Instrument Payloads onboard the Mars Exploration Rovers (MER) *Spirit* and *Opportunity* have provided new insights on the aqueous history at their respective landing sites in Gusev crater and Meridiani Planum. Measurements made with the Athena payload indicate that a variety of aqueous processes as well as various degrees of alteration have occurred at the two landing sites.

Aqueous alteration in Gusev crater ranges from minor alterations on the "plains" to highly altered materials in the Columbia Hills, which are located about 2.6 km to the southeast of the *Spirit* landing site. Light-toned rocks on the Gusev crater plains appear to have coatings or an alteration rind that may have resulted from limited aqueous alteration on the surfaces of basaltic rocks (*McSween et al*., 2004; *Haskin et al.*, 2005). Hematite and high $Fe^{3+}/Fe_{(total)}$ occur at the surfaces of some rocks (*Morris et al.*, 2004), and high concentrations of elements highly mobile in water (i.e., S, Cl, and Br) occur in rock veins, vugs, and coatings (*Gellert et al.*, 2004; *Haskin et al.*, 2005). Soil in trenches that were excavated with the rover's wheels exhibited stratigraphy higher in $Fe^{3+}/Fe_{(total)}$ ratios and mobile element concentrations (i.e., S and Mg) than surface soils, suggesting the translocation/transportation of these phases by water (*Haskin et al.*, 2005). Correlation between Mg and S suggest the formation of Mg-sulfates in these "mature" regoliths, possibly by the transportation of Mg and S by water and the subsequent evaporation of water and the precipitation of Mg and other sulfates (*Haskin et al.*, 2005). One scenario for the formation of rock coatings or rinds and translocation of mobile elements in Gusev crater is that thin films of water mobilized elements and hydrated rock surfaces, forming nanophase particles of iron oxides. These thin films of water might have occurred briefly at the Martian surface during periods of climatic change, e.g., changes resulting from diurnal and seasonal changes or during times of high obliquity (*Squyres et al.*, 2004a; *Yen et al.*, 2005).

Outcrops (layered and massive) and rocks on the West Spur of the Colombia Hills appear to be extensively altered as suggested by their relative "softness" as compared to crater floor basalts, high $Fe^{3+}/Fe_{(total)}$, iron mineralogy dominated by nanophase Fe^{3+} oxides, hematite and goethite, and high Br, S, and Cl concentrations beneath outcrop surfaces (*Morris et al.*, 2005; *Ming et al.*, 2005a,b). The discovery of goethite in West Spur outcrops is very important to

understanding the history of water in Gusev crater, because it can only form in the presence of water in contrast to hematite that can form by aqueous and non-aqueous processes. Positive correlations exist for Ca vs. S and for Mg vs. Cl, which suggest that the S and Cl phases in the outcrop materials may be Ca-sulfates, and Mg-chlorides (*Ming et al.*, 2005a,b). These outcrops and rocks undoubtedly formed by the alteration of basaltic rocks, volcaniclastic materials, and/or impact ejecta by solutions that were rich in volatile elements (i.e., Br, Cl, S) (*Ming et al.*, 2005a). However, it is not clear whether aqueous alteration occurred at depth (e.g., metasomatism), by hydrothermal solutions (e.g., associated with volcanic or impact processes), by aqueous vapors from volcanic emanations (i.e., acid fog weathering), or by low-temperature solutions moving through the West Spur materials. The layered outcrops on the West Spur of the Columbia Hills appear to be sedimentary in nature and deposited in a fluid, e.g., air fall deposits from volcanic ash or impact materials. Regardless of their emplacement process, liquid/vapor water had a major role in the alteration of outcrops and isolated rocks on the West Spur of the Columbia Hills.

The occurrence of jarosite ($(K,Na,H_3O)Fe_3(SO_4)_2(OH)_6$), other sulfates (e.g., Mg sulfates), and hematite along with siliciclastic materials in Eagle, Fram, and Endurance crater outcrops of sedimentary materials are strong indicators of aqueous processes at Meridiani Planum (*Squyres et al.*, 2004b; *Clark et al.*, 2005; *McLennan et al.*, 2005). Jarosite can only form by aqueous processes under very acidic conditions (*van Breeman*, 1980; *Bigham and Nordstrom*, 2000); e.g., acid-sulfate weathering conditions resulting from the aqueous oxidation of Fe sulfides (e.g., *Fernández-Remolar et al.*, 2005) or by sulfuric acid alteration of basalts by solutions associated with SO_2-rich volcanic gases (e.g., *Morris et al.*, 1996). It is plausible that acidic solutions rich in sulfur (and Fe^{2+} or Fe^{3+}) reacted with basaltic sediments to release their structural cations. Ferrous iron underwent oxidative hydrolysis to produce insoluble iron hydroxysulfates (e.g., jarosite) and oxides (e.g., hematite and goethite) and finally, through evaporation, formed siliciclastic sediments rich in other sulfates including those of alkali and alkaline earths cations (e.g., *Tosca et al.*, 2005). The Meridiani outcrops appear to have a complex diagenetic history as suggested by episodes of cementation and recrystallization, formation of hematite-rich spherules (interpreted to be concretions), and dissolution and formation of crystal mold vugs in outcrops (*McLennan et al.*, 2005). All of these diagenetic

features suggest water played an important role in formation of the Meridiani outcrop subsequent to the deposition of the sulfate-rich siliciclastic sediments.

Much of the aqueous alteration likely occurred early in the history of Mars. The outcrops at Meridiani represent the upper stratum of a complex sequence of layers that is dissected by Middle and Late Noachian cratered plains (*Arvidson et al.*, 2003); suggesting that these materials may have formed several billion years ago. The highly altered Columbia Hills are older than the flood basalts that cover the floor of Gusev crater near the landing site. The aqueous alteration may have occurred prior to the emplacement of the flood basalts of likely Hesperian age (*Golombek et al.*, 2003), suggesting that the alteration in the Columbia Hills may have occurred over 3 billion years ago.

The high abundance of S is obvious evidence that sulfate has played a major role in aqueous processes at both rover landing sites. The sulfate-rich outcrop at Meridiani Planum containing jarosite and Ca-Mg-sulfates has an SO_3 content of up to 25 wt. % (*Rieder et al.*, 2004; *Clark et al*., 2005). The interiors of rocks and outcrops on the West Spur of the Columbia Hills have up to 8 wt. % SO_3 (*Ming et al.*, 2005b). Soils at both sites generally have between 5 to 14 wt. % SO_3 (*Gellert et al.*, 2004; *Haskin et al.*, 2005). After normaliziation of major element compositions to a SO_3-free basis, the bulk composition of these materials are basaltic with exceptions in the Columbia Hills, suggesting the surface materials are derived from basaltic precursors by acid sulfate alteration. Several hypotheses have been suggested for the aqueous formation of sulfate-bearing phases on the surface of Mars including (1) the oxidative weathering of ultramafic igneous rocks containing sulfides (*Burns*, 1988; *Burns and Fisher*, 1990); (2) sulfuric acid weathering of basaltic materials (*Morris et al.*, 1996, 2000); and (3) acid fog (i.e., vapors rich in H_2SO_4) weathering of basaltic or basaltic-derived materials (*Clark and Baird*, 1979; *Banin et al.*, 1997). All three processes involve acid-sulfate weathering environments. Other candidate processes not involving acid sulfate conditions might include the dissolution and movement of soluble components by water (e.g., ground water, water thin films, flowing or standing water) and the subsequent formation of evaporitic minerals depositions, e.g., Mg- and Ca-sulfates and chlorides (*Moore et al.*, 1978, 1987; *Clark et al.*, 1982).

Although all of these candidate processes may have been important locally on Mars, we suggest that the primary alteration process is acid-sulfate, oxidative weathering of basaltic materials. Laboratory simulation weathering of basaltic materials under putative Mars-like

weathering conditions offers an important method to complement or supplement the MER observations in understanding the past (and present) aqueous processes on Mars (e.g., *Banin et al.*, 1997; *Tosca et al.*, 2004). The objective of this study is to conduct simulated Mars-like weathering experiments in the laboratory to determine the weathering products that might form during oxidative, acidic weathering of Mars analog basaltic materials. We have selected three possible oxidative sulfuric acid weathering environments to simulate: (1) sulfuric acid vapor (acid fog) weathering, (2) sulfuric acid weathering approximating an open hydrologic system, and (3) sulfuric acid weathering approximating a closed hydrologic system. Acid fog simulation was designed to maintain a very low water content, whereas the weathering experiments approximating open and closed systems were done at high water (high liquid:solid ratios) and high acidity contents at elevated temperatures to accelerate the process to achieve measurable results in a relatively short time.

2. Materials and Methods

2.1. Materials and Instrumental Methods

Two unaltered basaltic samples from the Island of Hawaii were used as starting materials for the acid sulfate weathering experiments. One sample was an olivine-rich sand (HWPC100) obtained from the Puna Coast. The second sample was a plagioclase-rich tephra (HWMK725) obtained from near the summit of Mauna Kea Volcano. A Scintag XDS 2000 X-ray diffractometer using Cu-Kα radiation operated at 45 kV and 40 mA current was used to characterize the mineralogy of random powder mounts over the range of 2 to 70^{o} 2θ. Morphological, mineralogical, and chemical properties of the basaltic samples were characterized by a JEOL 5910LV scanning electron microscope (SEM) equipped with an energy dispersive spectroscopy (EDS). Quantitative chemical analyses of phases in polished sections were conducted by EDS analysis using a 100 nm beam, 15kV acceleration voltage, 10 mm sample working distance, and detector at a 35^{o} angle. Calibration standards of olivine and plagioclase were used for ZAF corrections of the respective phases. Major element chemistry of starting materials was determined by X-ray fluorescence (XRF) spectroscopy using a 9:1 $Li_2B_4O_7$-sample flux-fusion procedure to prepare glass disks and a Philips 2404 XRF spectrometer equipped with a 4 KW Rh X-ray tube (see *Boyd and Mertzman*, 1987). Transmission Mössbauer spectra were obtained at room temperature (~293 K) on Ranger

Scientific spectrometers (*Morris et al.*, 1985, 1989, 2000). Absorbers for transmission experiments were made by dispersing powdered samples (<150 μm) in epoxy to a density of 50-100 kg/m^2 of Fe. Mössbauer parameters, derived by fitting folded spectra to theoretical line shapes using an in-house computer program (JSCFIT), are the isomer shift (IS) relative to the midpoint of the spectrum of metallic iron foil at 293 K, quadrupole shift (QS), hyperfine field strength (B_{hf}), and line widths (W).

2.2. Acid-Sulfate Weathering Experiments.

2.2.1. Sulfuric Acid Vapor (Acid-Fog) Reactions

Samples were prepared in two ways: (1) polished thick sections of natural particles and (2) natural ("as is") particles (0.5-1.0 mm). For polished thick sections, "as is" basaltic particles were embedded in epoxy, mounted on a glass slide, and only the exposed surface was polished. Polished sections were examined by SEM backscatter imaging and EDS analysis prior to sulfuric acid vapor weathering experiments. A 23-mL Teflon-lined hydrothermal vessel (Parr® bomb) was half filled with 4-mm diameter quartz-glass beads. Two mL of concentrated H_2SO_4 was placed at the bottom of the reactor. Thick sections were placed with sample side up on top of the quartz-glass beads, well above the concentrated H_2SO_4. The Teflon-lined container was closed tight and placed inside a stainless steel casing and heated to 145^{o}C in an incubator oven for 144 hours. At the end of the experiment the containers were cooled to room temperature and opened to recover the exposed section. The boiling point of H_2SO_4 is 338ºC at which the vapor pressure is 101.3 kPa. The vapor pressure at 145ºC is extremely low (~ 0.004 kPa); hence, appreciable quantities of sulfuric acid vapor are not expected to condense as bombs were cooled to room temperature during the recovery of reaction products. Sections were stored at 56 % relative humidity (RH) for 72 hours and then carbon coated prior to SEM analysis. A blank epoxy thick section (no sample) treated similar to the sample thick sections showed that Si from quartz beads did not contaminate surfaces of thick sections although epoxy became brittle and dark after the treatment.

In separate experiments, granular basaltic particles were exposed to hot sulfuric acid vapors (145ºC) in a closed vessel in a similar fashion to the polished thin sections as described above, except that basaltic particles were placed on a small platinum dish, which was placed on

the glass beads. At the end of the experiment the particles were recovered and immediately characterized by X-ray diffraction (XRD) analysis. Particles not used for the XRD analysis were stored at 56% relative humidity (RH) for 72 hours and characterized again by XRD analysis. Samples stored at 56 % RH were C-coated. The morphology and chemistry of C-coated samples were characterized by SEM and EDS analyses.

2.2.2. Oxidative Sulfuric Acid alteration of Basalt in a Three-step Batch Experiment Approximating an Open System

An open hydrologic system was approximated by placing 100 mg of basaltic materials, 10 mL of 0.45 M sulfuric acid solution, and 2 mL of 31% H_2O_2 in a Teflon-lined vessel incased in a stainless steel bomb (~9 mg of O_2 was added per mL of solution). Hydrogen peroxide was chosen as the oxidizing agent because superoxides and peroxides have been suggested as candidates for the purported oxidant in Martian surface materials (e.g., *Zent and McKay*, 1994), and it will not cause appreciable change in ionic strength or alkalinity of leaching solutions. Two particle sizes were used for individual experiments: (1) 0.5-1.0 mm; and (2) < 53 μm formed by completely grinding the 0.5-1.0 mm fraction to pass through a 53-μm sieve (ground materials will have more reactive surface area). Reaction vessels were placed into an incubator oven and heated to 145ºC for 48 hours and then cooled to room temperature before removing the reactants from the Teflon containers. Solids were separated from the solution by carefully decanting the solution. A 2-mL portion of the solution was saved for chemical analysis (leachate OS-1). Two mL of H_2O_2 (31%) was added to the remaining leachate and transferred into a second Teflon-lined reaction vessel containing 100 mg of fresh basaltic materials. The reaction vessel was heated to 145ºC for 48 hours. Samples and solutions (leachate OS-2) were separated as described above. This procedure was repeated a third time (leachate OS-3). Solid residues from each step were saved in a -20ºC freezer to arrest any further reaction and freeze-dried for XRD, SEM, EDS, and Mössbauer analyses and leachate samples (leachates OS-1, OS-2, and OS-3) were centrifuged at 10,000 rpm for 10 min in a IEC-B-22 Centrifuge to remove particulates and analyzed for Na, K, Ca, Mg, Si, Al and pH. A GBC 903 Atomic Absorption Unit was used to measure solution Na, K, Ca, Mg, Si, and Al. The samples were again centrifuged for longer time periods and analyzed for Na, K, Ca, Mg, Si, and Al. Si appeared to decrease suggesting that it

was in a colloidal state $(H_2SiO_4)_n$; however, the other elements did not change indicating that they were in solution.

The procedure described above is an approximation for an open system because the starting material is refreshed and the leachate solutions are reused at each step, increasing the concentration of dissolved species (e.g., *Barth-Wirsching et al.*, 1990).

2.2.3. Oxidative Sulfuric Acid Alteration of Basalt in a Single-step Batch Experiment Approximating a Closed System

A closed hydrologic system was approximated by placing 100 mg basalt (0.5-1.0 mm), 10 mL of 0.45 M sulfuric acid solution, and 6 mL of H_2O_2 (31%) in a Teflon-lined stainless-steel vessel (~27 mg O_2 was added per mL of solution). The reaction vessel was heated at 145ºC for 144 hours. Residues and the final leachate (leachate CS) were analyzed at the end of the experiment as described above for the three-step leaching experiments.

Here we define a "closed system" as any system where reactants are added to the system (i.e., volatile phases such as S, Cl, and Br) and no products (except water and other gaseous phases via evaporation) are transported out of the system during or after the reaction. Perhaps there is rarely a natural system that approaches a perfect closed system (i.e., no additions and no losses), but it is used here for comparison with the three-step leaching experiments.

3. Results

The relative abundance of phases in HWPC100 basaltic sand is olivine > glass > plagioclase feldspar > pyroxene > titanomagnetite (Fig. 1). Olivine in HWPC100 is Mg-rich ($Fo_{80}Fa_{20}$) as estimated by EDS analysis of representative olivine grains. The relative abundance of phases in HWMK725 basaltic tephra sample is glass > plagioclase feldspar > olivine> titanomagnetite (Fig. 2). Plagioclase feldspar in HWMK725 was Ca and Na rich ($Ab_{50}An_{46}Or_4$). HWMK725 is more Al and Si rich than any Martian meteorite and represents an extreme possible composition on Mars; whereas HWPC100 is similar in chemistry to the "Peace" outcrop on the northwest flank of Husband Hill in the Columbia Hills of Gusev crater (Ming et al., 2005b). Bulk compositions (XRF analysis) of starting materials reflect the high Mg in olivine for HWPC100 and high Al and Na in plagioclase feldspar for HWMK725 (Table 1).

Secondary phases that formed after exposure to sulfuric acid weathering conditions for acid fog, three-step, and single-step batch leaching experiments are listed in Table 2. Products identified by XRD analyses immediately after experiments ended and after exposure to 54% RH for 72 h are listed to illustrate that crystallinity and hydration state for Mg, Ca, and Al sulfates depend on environmental conditions. Details on the identification and characterization of weathering phases for each starting material are described next.

3.1. Olivine-Rich Basaltic Sand HWPC100

3.1.1. Sulfur Acid Vapor Reactions of Basalts: Natural Particles

X-ray amorphous magnesium sulfates formed as reaction products after HWPC100 olivine-rich basalt particles were exposed to the sulfuric acid vapors. X-ray amorphous magnesium sulfates were assumed to have initially formed because of the absence of peaks in XRD diffractograms for samples that were analyzed immediate after the vessel was cooled as compared to samples exposed to 54% RH where hexahydrite ($MgSO_4 \cdot 6H_2O$) was identified as the only secondary alteration phase (Fig. 3). SEM and EDS analysis indicated that HWPC100 particles were coated mostly by Mg-sulfates and similar to phases that formed on polished surfaces (see Supplemental Figure 1).

3.1.2. Oxidative Sulfuric Acid Vapor Reactions of Basalts: Polished Thick Sections

Polished thick sections exposed to sulfuric acid vapors permitted observation of the extent phases in the original basaltic materials altered and the phases that formed on their surfaces (Fig. 4). Glass appeared to be the least reactive phase in the HWPC100 sample; plagioclase feldspar was more reactive as suggested by etch features and abundant Ca-sulfate crystals associated with plagioclase feldspar (Fig. 4). The glass's apparent resistance to alteration may be a factor of reaction kinetics due to particle size, i.e., glass particles are larger than the plagioclase particles. Olivine was the most reactive phase in HWPC100; in many cases the olivine was completely replaced by Mg sulfates (Fig. 4d). Ca-sulfate crystals readily formed on much of the surfaces of basaltic sand grains after exposure to sulfuric acid vapors. Most Ca-sulfate crystals were <2 μm in size (Fig. 4a,b), while a few large gypsum crystals (25-50 μm) were also found near grain surfaces (Fig 4a). Olivine underwent intensive alteration and leaching leaving an amorphous silica residue and $MgSO_4.nH_2O$ on crystal surfaces (Figure 4d).

Magnesium sulfate is the most abundant salt observed in the olivine-rich basalt; however, the highly hydrated Mg-sulfate crystals were difficult to image by SEM because of their instability in the microscope's electron beam and vacuum. Alunogen ($Al_2(SO_4)_3 \cdot 17H_2O$) was a rare product after alteration of HWPC100. Alunogen was identified by EDS analysis (Al and S) and their plate-shaped crystal morphology (see below). In summary, phases formed by acid-fog alteration of HWPC100 were $MgSO_4 \bullet nH_2O$, Ca-sulfates (gypsum and probably anhydrite), amorphous silica, and minor alunogen.

3.1.3. Oxidative Sulfuric Acid Alteration of Basalts in Three-step Batch Reaction Experiments Approximating an Open System

Unreacted basaltic sand HWPC100 was rich in olivine and glass with small amounts of plagioclase feldspar, pyroxene, and titanomagnetite. Starting materials for experiments were the 0.5-1.0 mm and <53 μm size fractions of HWPC100. For both starting materials, the olivine completely reacted in the first leaching as shown by the absence of XRD peaks for olivine (Fig. 5). Only relatively acid resistant plagioclase feldspar and some pyroxene remain as the mineral phases in the residues after the first 48-hour treatment. Fe and Ca sulfates formed as reaction products after the second and third leaching steps for both 0.5-1.0 mm and <53 μm starting materials (Fig. 5). The XRD mineralogy of these sulfates phases was jarosite, gypsum, and anhydrite (note: anhydrite was only detected by XRD analysis in the <53 μm material, see Supplemental Figure 2). Very broad peaks at around 4 Å d-spacing (18-32 º2θ) suggested the formation of amorphous silica as an alteration product of HWPC100 (Fig. 5). Jarosite, gypsum, and Mg sulfate crystals were observed in SEM images (Fig. 6c,d). The jarosite is a hydronium-sodium variety [$(H_3O)_{0.95}Na_{0.05}Fe_3(SO_4)_2(OH)_6$)] as suggested by the low Na and trace K compositions as measured by EDS.

The Mössbauer spectra for untreated and treated HWPC100 samples are compared in Fig. 7. The oct-Fe^{2+} olivine doublet is no longer present in the treated sample, in agreement with the absence of the phase in XRD data. The oct-Fe^{3+} in the treated sample is assigned to jarosite and supports the XRD analysis. Although the olivine has been completely altered, the glass has not as shown by the presence of the oct-Fe^{2+} doublet from glass. No magnetic or nanophase oxide phases were detected. A MB spectrum of sulfatetic tephra sample HWMK515 from near the summit of Mauna Kea Volcano in Hawaii (*Morris et al.*, 2000) is shown for comparison in Fig.

7. The spectra for the sulfuric acid treated HWPC100 and natural HWMK515 are remarkably similar. HWMK515 likely formed when hydrothermal solutions enriched in sulfuric and hydrochloric acids (volcanic in origin) percolated through tephra materials (*Morris et al.*, 2000).

3.1.4. Sulfuric Acid Alteration of Basalts in a Single-step Batch Experiment Approximating a Closed System

Starting material for these experiments were the same as for the three-step reaction experiments discussed above. Only plagioclase feldspar and pyroxene remained as residual mineral phases in the single-step experiment residue after sulfuric acid treatment of HWPC100 starting materials (Fig. 5). A very broad peak at ~4 Å d-spacing (18-32 $^{o}2\theta$) suggests the formation of amorphous silica as an alteration product.

Scanning electron micrographs of acid-sulfate treated HWPC100 particles showed leached glass surfaces; however, the morphology of the original glass shard was maintained (compare unaltered glass shard in Fig. 6a to altered glass shard in Fig. 6b). The olivine has been completely dissolved while leaving behind a precipitate of amorphous silica on particle surfaces (Figure 6b). The amorphous silica phase was assumed based upon the XRD analysis (see above) and the high Si content at the surface as detected by EDS analysis.

3.2. Plagioclase Feldspar-Rich Basaltic Tephra HWMK725

3.2.1. Sulfuric Acid Vapor Reactions of Basalts: Natural Particles

Particles of plagioclase-rich basalt HWMK725 were partially altered upon exposure to sulfuric acid vapors. Reaction products analyzed immediately after treatment were transient Al and Fe sulfate phases; the peaks marked T1-T4 in Fig. 8 are assigned to aluminum hydrogen sulfate ($AlH(SO_4)_2$) and an anhydrous iron sulfate (X-ray powder diffraction file - PDF: 21-0922). After exposure to ambient conditions (RH ~ 56 %) for 72 hr, XRD peaks were present that corresponded to alunogen, hexahydrite, and voltaite ($K_2Fe_5Fe_4(SO_4)_{12}.18H_2O$) (Fig. 8). Presumably, these crystalline salts formed by hydration and reprecipitation of initially X-ray amorphous and transient phases.

In SEM images and by EDS analysis, Al- and S-rich platy crystals were observed adhering to individual grains of HWMK725; the play crystal morphology was similar in morphology to platy crystals that formed on surface of thick sections after exposure to sulfuric

acid vapors (see below). Presumably, these crystals correspond to the alunogen detected by XRD analysis. Halite crystals were also observed in SEM images of reacted HWMK725, indicating the presence of Cl-bearing phases that were present in the original starting material (see Table 1). These samples were not washed after residues were separated from the reacting solutions; hence, the halite formed during the evaporation of small amounts of aqueous solution remaining with the residue.

3.2.2. Oxidative Sulfuric Acid Vapor Reactions of Basalts: Polished Thick Sections

Etched (or leached) olivine surfaces in HWMK725 thick sections show that olivine is extensively altered after exposure to H_2SO_4 vapor (Fig. 9b). Plagioclase feldspar and glass appear to be etched less (Fig 9bc).

Although not seen in the XRD analysis of the acid vapor treated natural grain samples (section 3.2.1), nearly all polished surfaces of HWMK725 thick sections were decorated with Ca sulfate crystals of 1-2 μm in size (Fig. 9). The Ca sulfate appears to be crystalline, although it was difficult to differentiate the crystal habit (i.e., differentiate anhydrite and gypsum) because of their small sizes. Models of our hydrothermal system suggest that anhydrite would be the stable phase to form above 40ºC, and therefore at 145ºC anhydrite would be the expected phase. In some instances, Ca sulfate crystals appeared to be more abundant on the plagioclase feldspar crystals (Fig. 9c). However, there were tephra particles where glass appeared to have undergone greater leaching as suggested by the abundance of Ca sulfate crystals on their surfaces (Fig. 9d). The surface precipitation of Ca sulfate appears to be a function of the amount of Ca in the phase being leached, i.e., more Ca sulfate nucleated at the surfaces of particles with high Ca contents (e.g., plagioclase feldspar, pyroxene or glass with high Ca contents). Surfaces of nearly all tephra particles were covered with amorphous Si as suggested by the detection of high Si by EDS analysis. Plate-shaped alunogen was found in abundance near the surfaces and edges of grains (Fig. 9a). Alunogen formation near the grain-epoxy interface suggests migration of solvated Al^{3+} along grain surfaces and subsequent nucleation at the surface. Alunogen plates were occasionally found lying flat on glass surfaces, although, most basaltic grain surfaces were not impregnated by the Al sulfate. In summary, the primary phases that formed on the surfaces of HWMK725 were Ca sulfate, alunogen, and amorphous silica.

3.2.3. Oxidative Sulfuric Acid Alteration of Basalts in Three-step Batch Reaction Experiments Approximating an Open System

The XRD analysis (Fig. 10) of solid phases from the three-step leaching experiments for HWMK725 shows plagioclase feldspar as the predominant residual mineral after each step for both starting materials (0.5-1.0 mm size fraction and for <53 μm powder of bulk sample). A broad, weak intensity peak between 18-32 º2θ was assigned to amorphous silica.

3.2.4. Sulfuric Acid Alteration of Basalts in a Single-step Batch Reaction Experiment Approximating a Closed System.

The XRD pattern of solid phases from the single-step batch experiment HWMK725 shows that plagioclase feldspar is the predominant residual mineral for both particulate starting materials (Fig. 10). The broad hump near 4 Å d-spacing (18-32 º2θ) is more intense than for residual phases in the three-step leaching experiments, suggesting that a higher proportion of amorphous silica is present as an alteration phase.

4. Aqueous chemistry of simulated sulfuric acid weathering environments.

The experiments with three steps of leaching allow simulation of solutions moving through the basalt, dissolving ions and transporting them to other locations. Precipitation of phases from solution depends on the degree of solution saturation with respect to the forming phase, solution pH (i.e., degree of neutralization of acidic solutions) and the activity of water (e.g., degree of evaporation of solutions). The single-step and the sulfuric acid fog experiments simulate isochemical alteration (i.e., closed system alteration except with respect to input of the acid-sulfate alteration agent). Cations are not leached from the system.

The three sequential leaching steps that simulated the open system allowed for oxidation and evaporation of acidic solutions between steps. Cation concentrations in leachates increased as the leaching solution scavenged more cations and the acidity was neutralized by fresh basalts in each step for both HWMK725 and HWPC100 (Fig. 11a,b). The relative concentrations of cations were different in extracts of olivine-rich basalt versus plagioclase feldspar-rich basalt. Leachate compositions were controlled by the composition of the most soluble components in each sample. Mg and Fe concentrations were higher in HWPC100 leachates where olivine (~$Fo_{80}Fa_{20}$) is a major component (Fig. 11a,b). The complete dissolution of the olivine in 0.45

M H_2SO_4 in HWPC100 is consistent with the susceptibility of olivine to acid attack (e.g., *Grandstaff*, 1986; *Wogelius and Waltheral*, 1992) and likely accounts for the very high Mg level observed in the HWPC100 leachate. Although the Fe and K concentrations are relatively low in the three-step leachate for HWPC100 (Fig. 11b), they formed insoluble jarosite (very low K_{sp}) in the presence of acidity and sulfate anions (e.g., Baron and Palmer, 1996). K incorporation into the jarosite is suggested by the decrease in K concentration for the OS-2 and OS-3 leachates as compared to the OS-1 leachate (Fig. 11b). Al and K concentrations are higher in the HWMK725 because plagioclase feldspar (~$Ab_{50}An_{46}Or_4$) is a major component contributing cations into solution (Fig. 11a,b).

The pH of the solution increased in the three-step experiment as the leachate passed through each batch of basalt (Figs. 11c,d). The pH rise in the HWPC100 leachates was larger than the pH rise in HWMK725 leachates. The pH rise in the olivine-rich leachate might suggest that the acid neutralization by olivine was much more effective than that by plagioclase feldspar. One factor may be the release of Mg^{2+} in olivine, compared to Al^{3+} in plagioclase feldspar. The Al^{3+} cation is an acid producing cation compared to neutral Mg^{2+} (e.g., *Banin et al.*, 1997). Silica (silicic acid) has a very high pK1 value (9.49, *CRC Handbook of Chemistry and Physics*) and is able to sequester H^+ ions causing the pH to rise; hence, the higher Si concentration may also contribute to the pH rise in HWPC100 solutions.

The leaching of Ca, Mg, Na, K, Al and Fe in the single-step batch experiment was similar to the leaching of cations in the three-step leaching experiment, except that the total cation concentrations in the 3rd leachate in the three-step leaching experiment were higher than for the single-step leachate (Fig. 11a,b). The secondary mineral precipitation was limited to amorphous silica for both basaltic materials in the single-step leaching experiments.

It is important to note differences between the results for the three-step and single-step leaching experiments may be a kinetic effect and/or a consequence of different water to rock ratios. Focusing on only HWPC100 experiments, the extent of dissolution may become limited by kinetics once the near surface regions of the particles have been leached. If so, this would limit the availability of cations, particularly from the glass, and not permit the Fe^{3+} concentration to be sufficiently high to precipitate jarosite. Jarosite may not have formed in the single-step leaching experiment because the water to rock ratio in our experiments was sufficiently high that the aqueous solutions were undersaturated with respect to jarosite precipitation and the pH did

not rise into the jarosite stability field (see below). Therefore, we cannot exclude jarosite formation in a closed system if environmental conditions permit exceeding the solubility product of the sulfate. The water to rock ratio cannot be too low, however, or the basalt will buffer the pH a value above that required for jarosite precipitation.

The release of ions for ground starting materials (<53 μm powders) and the alteration products that formed were similar to the experiments conducted with 0.5-1.0 mm materials. As would be expected, the increased surface area did result in slightly higher concentrations of elements into solution. The 0.5-1.0 mm sized material better represent eolian basalt sands that may have been present and subsequently altered on Meridiani Planum (see discussion below). Solutions were not collected for the acid fog experiments because of the near absence of water in the system. Amorphous silica, Ca sulfates, alunogen, and amorphous Mg-sulfates formed at the surfaces of polished thick sections of the Mars analog basaltic particles after exposure to sulfuric acid vapor. This suggests that Si, Ca, Mg, and Al were released into "solution" and migrated to the surface where they reacted with H_2SO_4 (aq) to form various sulfates along with amorphous silica.

5. Discussion

5.1. Acid Fog Weathering

Aluminum, Mg, Ca, and Fe sulfates and amorphous silica are the phases that formed after basaltic tephra and sand were subjected to oxidative, sulfuric acid vapors in our experiments. These results are consistent with the experimental results of *Banin et al.* (1997) and *Tosca et al.* (2004). Laboratory simulated acid weathering of palagonitic tephra resulted in the formation of gypsum and alunogen (*Banin et al.*, 1997). They hypothesize that the top layer of Mars "soil" may have formed by extremely slow ongoing weathering interactions at the atmosphere-rock interfaces. The reactions are driven by acidic volatiles (e.g., SO_2, Cl) deposited from the atmosphere and then reacted with the mineral surfaces in the dry Mars environment. Tosca et al. (2004) subjected synthetic basaltic analogs derived from Mars Pathfinder soil and rock compositions to various acidic solutions and subsequent evaporation. Crystalline Mg, Fe, Ca, and Al sulfates (but not jarosite) were identified as reaction products along with the formation of secondary ferric oxide phases, which formed via rapid Fe oxidation under relatively high pH levels buffered by basalt dissolution. Amorphous silica was also identified as a ubiquitous product on particle surfaces.

A major difference between the studies of *Banin et al.* (1997) and *Tosca et al.* (2004) and our experiments is that we did not react the basaltic materials in solution, but instead sulfuric acid vapors interacted with the materials that maintained the activity of water near zero. Another important difference is that we preformed experiments under hydrothermal conditions (145ºC) compared to experiment temperatures near 25ºC for *Banin et al.* (1997) and *Tosca et al.* (2004). Our goal was to create environmental conditions where sulfuric acid vapors reacted with basaltic materials without any leaching of solutions and the higher temperatures simulated hydrothermal conditions as well as enhance the kinetics of dissolution and neoformation of sulfates. Small amounts of water inherent to the basaltic samples used in our experiments and in the concentrated sulfuric acid will contribute to the activity of water, but the water either reacted with the basaltic materials to form hydrated phases or was lost by evaporation when exposed to room temperature conditions after opening hydrothermal vessels.

Amorphous or transient sulfates appear to form first in our acid fog experiments with a very low water activity. Crystalline sulfates formed after exposure to ambient conditions (RH ~ 54 %). No doubt, RH has a major role in controlling the mineralogy of hydrous sulfates. This is especially the case for the Mg sulfates where modest changes in the RH will result in different hydration states or mineralogy (e.g., *Vaniman et al.*, 2005). It is plausible that acid fog weathering on Mars resulted in the formation of amorphous sulfates; these sulfates may still be amorphous, depending on the subsequent interaction of water (e.g., atmospheric) with the sulfates and the amount of water within the surface materials. New data currently being acquired by the OMEGA instrument onboard the Mars Express orbiter may provide new insights on the sulfate mineralogy on Mars (*Bibring et al.*, 2005; *Gendrin et al.*, 2005; *Langevin et al.*, 2005).

5.2. Three-step Leaching Experiments Approximating an Open System

Jarosite, Mg, and Ca sulfates and amorphous silica formed from the olivine-rich basaltic sand and amorphous Si formed from the plagioclase-rich basaltic tephra during acid-sulfate alteration in three-step (hydrothermal) leaching experiments. The formation of jarosite is analogous to the formation of jarosite in basaltic materials on Mauna Kea volcano in Hawaii under oxidizing, hydrothermal conditions (*Morris et al.*, 1996, 2000). The sulfuric acid solutions were thought to be a result of interactions of SO_2–rich volcanic gases. Acid sulfate solutions percolated up through the basaltic tephra, dissolved Fe and other cations, and precipitated

jarosite when environmental conditions permitted its formation. The Fe mineralogy of some Mauna Kea sulfatetic tephra is very similar to the Fe mineralogy in our three-step leaching experiments of the olivine-rich basaltic sands used in these experiments (see Fig. 7)

In several cases, hematite occurred with the jarosite in Mauna Kea sulfatetic tephra, suggesting that Fe oxide either co-precipitated with the jarosite under hydrothermal conditions or they are hydrolysis products of jarosite dissolution. The pH of the system plays a major role in defining the stability field between jarosite and hematite (or goethite). The pH values in our experiments were lower than 1 in most cases (Fig. 11c,d); Fe^{3+} likely remained in solution at these low values. Jarosite only precipitated in the three-step leaching experiments (OS-3); which had the highest pH values (Fig. 11c,d). Jarosite is stable in the pH range ~0.75-3.5; below this range jarosite dissolves and above this range it hydrolyzes to form hematite and/or geothite (e.g., stability diagram in *Burns and Fisher* (1990)). Thus, in our three-step leaching experiments, pH values were not high enough to initiate jarosite dissolution and subsequent hydrolysis of Fe to form Fe oxides or oxyhydroxides (e.g., hematite, goethite). We surmise that if we repeated our three-step leaching protocol enough times that the continued dissolution of basaltic materials would neutralize the acidity until the pH of the system favored the formation of iron oxides and oxyhydroxides.

5.3. Single-step Batch Reaction Experiment Approximating Closed Systems

Only amorphous Si formed under single step experiments. Apparently, the closed system solutions did not achieve supersaturation with respect to ferric sulfates, such as jarosite. Movement of solutions through basaltic materials (i.e., open hydrologic systems) allows for the neutralization of the acid by the dissolution of basaltic components. The inability of the basalt to neutralize the closed system solutions limited the formation of phases such as jarosite (which is soluble at very low pH), but Si reached saturation with respect to the formation of amorphous silica. If the solid to solution ratio was lower in our experiments, then it may have been possible to form jarosite and other sulfates. We did not test a range of solid:solution ratios; hence, we cannot rule out the possibility of forming jarosite in a closed system.

6. Implications for Sulfate Formation on Meridiani Planum

Jarosite, hematite, and other sulfates (e.g., Mg sulfates) occur along with siliciclastic sediments in outcrops at Meridiani Planum. A leading candidate for the formation of these sediments is the evaporation of acid fluids that have interacted with and altered olivine-bearing basaltic materials (*Tosca et al.*, 2005). A key but reasonable assumption is that waters rich in sulfuric acid interacted with basaltic sediments in Meridiani Planum. Sulfuric acid waters could form by the interaction of volcanic emissions (i.e., SO_2, Cl, Br) with water vapor or liquid. Key questions on the formation of these sulfate-rich sediments are how much acidic water interacted with the basaltic sediments and whether solutions moved through these sediments and removed soluble constituents (i.e., open hydrologic system) or if these sediments were altered under isochemical conditions (i.e., closed hydrologic system).

Based upon our experiments, the formation of jarosite in the Meridiani outcrops may reflect only slight neutralization of acidity to move the Fe^{3+} ion into the jarosite stability field, similar to what we observed in our three-step leaching regime. Waters rich in sulfuric acid (e.g., ground water) may have moved through basaltic sediment and dissolved olivine-rich basaltic phases in the sediments. Dissolved Mg, Ca, Na, K, and residual Fe^{3+} were transported causing further neutralization of the solution to precipitate iron oxides. Gypsum (or anhydrite) was one of the sulfates to initially precipitate because of its low solubility while other alkali metal and alkaline earth sulfates precipitated during further evaporation of solutions (e.g., *Tosca et al.*, 2005). This type of weathering is supported by the occurrence of jarosite and the dearth of olivine (oct-Fe^{2+} in olivine as detected by MB (*Klingelhöfer et al.*, 2004)) in the siliciclastic sediments. There is some oct-Fe^{2+} in Meridiani outcrop that is interpreted as pyroxene (*Klingelhöfer et al*., 2004). If so, the pyroxene is more resistant than olivine to attack by sulfuric acid. Although there is only indirect chemical evidence for feldspar in Meridiani sediments (*Clark et al.*, 2005), the phase would also be more resistant to alteration than olivine based on our three-step leaching experiments. This mineralogical description is similar to that for our three-step leaching of HWPC100 where jarosite formed at the expense of olivine dissolution and plagioclase feldspar remained as the primary residual phase. By implication, the Meridiani outcrop could have formed by a similar process. A possible caveat is that the bulk composition of the outcrop may not be compatible with significant additions of Fe, Mg, and other cations accompanying acid sulfate solutions. Alternatively, our experimental open-system conditions could be mimicked by a closed system process on Mars where the composition of the basaltic

precursor and water to rock ratio were favorable for dissolution of silicate Fe^{2+} under acid-sulfate conditions to soluble Fe^{3+} and subsequent precipitation of jarosite and other phases when their solubility products become exceeded by, for example, partial neutralization of acid sulfate solutions during dissolution of basic basaltic materials.

The Meridiani outcrop contains two populations of hematite; fine-grained hematite dispersed within the outcrop matrix and hematite-rich spherules (1-6 mm) embedded in the outcrop (*Klingelhöffer et al.*, 2004; *Herkenhoff et al.*, 2004). Possible hematite formation processes are covered in detail by *Tosca et al.* (2005) and *McLennan et al.* (2005). In their view, insoluble sulfates (e.g., jarosite) and evaporate type minerals form first in acid sulfate weathering environments. Iron oxide formation is the result of oxidative hydrolysis of Fe that occurs as the pH increases in response to acid neutralization by the reaction with basic basaltic materials. Although we did not form iron oxides or oxyhydroxides in our short-term experiments, it is possible that their formation was precluded because our acidic solutions were not allowed to react long enough to neutralize the acidity and raise the pH into the stability field for hematite or goethite.

7. Implications for Sulfate Formation in Gusev Crater

Evidence for aqueous alteration processes involving S, Cl, and Br range from minimal for rocks on the Gusev plains to extensively altered outcrops and rocks in the Columbia Hills. Specific S, Cl, or Br minerals have not been identified by the mineralogical instruments onboard the *Spirit* rover, unlike the identification of jarosite in Meridiani outcrops. Chemical compositions (APXS data) and Fe mineralogy and oxidation state (Mössbauer spectrometer data), however, are being used to constrain the possible mineralogy of these volatile-bearing phases. For example, the positive correlation of Mg and S in some Gusev soil trenches suggests the mobilization and precipitation of Mg-sulfate phases (*Haskin et al.*, 2005). More extensive alteration appears to have occurred in the Columbia Hills where some outcrops have high S, Cl, and Br in subsurface rock that was exposed by the Rock Abrasion Tool (RAT). Positive correlations between Ca and S in some outcrops (e.g., "Clovis") suggest the occurrence of Ca-sulfates (*Ming et al.*, 2005a,b). Recently, the *Spirit* APXS has detected high Mg and S concentrations in several outcrops (e.g., "Peace") that suggest the possible occurrence of Mg-sulfates (Ming et al., 2005b).

Acid-sulfate weathering is a leading candidate process for the formation of the purported occurrence of Mg and Ca-sulfates in the Columbia Hills. Most of the outcrops examined by APXS on the West Spur of the Columbia Hills exhibit small differences in the primary rock forming elements Al, Si, and Fe. The major differences are the oxidation state of Fe, Fe-bearing phases, and especially the amounts of S, Cl, and Br when compared to the olivine-rich basalts on the "plains" of Gusev crater near the landing site. The aqueous alteration in these materials may be isochemical weathering under closed hydrologic systems or acid fog conditions. The major products in our acid fog weathering experiments were alunogen, Mg-sulfates, Ca-sulfates, and amorphous Si. There have been no suggestions (e.g., APXS correlations of Al and S) for alunogen or Al-sulfate formation in the West Spur rocks or outcrops. Amorphous Si is a common product of the sulfuric acid weathering of basaltic materials; however, secondary silica has yet to be identified in the Columbia Hills. The possible occurrence of Ca- and Mg-sulfates suggests sulfuric acid weathering of basaltic materials that may have been rich in olivine, pyroxene and plagioclase feldspars. This hypothesis is supported by the low abundance of olivine in the West Spur outcrops and rocks as determined by MB (*Morris et al.*, 2005). Oct-Fe^{2+} interpreted as pyroxene is detected in outcrop rocks at levels comparable to rocks in the Gusev plains. Plagioclase feldspars are likely phases in some of the Columbia Hills outcrops, but their occurrence has not yet been made by direct mineralogical measurements by MER instruments; only assumed by APXS normative chemical calculations (Ming et al., 2005b).

One scenario for aqueous alteration on the West Spur is that vapors rich in SO_2, HCl, HBr, and water interact at surfaces of rocks and outcrops, which are basaltic in bulk composition and are presumably volcaniclastic or impact deposits (*Ming et al.*, 2005a,b). Acidic vapors diffused into the rocks and outcrops and react with the primary phases (mainly olivine). Soluble ions from the host rock reacted with S (and likely Cl and Br) to form Ca-, Mg- and other sulfates along with iron oxides and oxyhydroxides.

Although the experimental results presented here are used to support or strengthen the current knowledge of the Martian surface processes, a caveat is that the knowledge bank is still evolving and any conclusions drawn here can only be firmly validated by more in-depth mineralogical and geochemical characterization of martian surface materials (e.g., 2009 Mars Science Laboratory Mission, Mars sample return missions, etc.).

Acknowledgements

This work was funded by the NASA Mars Fundamental Research Program through a grant to DWM. We thank Ben Clark and an anonymous reviewer for their very helpful reviews.

References

Arvidson, R. A., F. P. Seelos, IV, K. S. Deal, W. C. Koeppen, N. O. Snider, J. M. Kieniewicz, and B. M. Hynek, M T. Mellon, and J. B. Garvin, Mantled and exhumed terrains in Terra Meridiani, Mars, *J. Geophys. Res*., *108*(E12), 8073, doi:10.1029/2002JE001982, 2003.

Banin, A., F. X. Han, I. Kan, and A. Cicelsky, Acidic volatiles and the Mars soil. *J. Geophys. Res., 102,* 13,341-13,156, 1997

Baron, D., and C. D. Palmer, Solubility of jarosite at 4-35°C, *Geochim. Cosmochim. Acta, 60,* 185-195, 1996.

Barth-Wirsching, W. U., R. Ehn, H. Hoeller, D. Klammer, and W. Sitte, Studies on hydrothermal alteration by acid solutions dominated by SO_4^{2-}: Formation of the alteration products of Gleichenberg latitic rock (Styria,Austria); experimental evidence, *Mineral. Petrol., 41,* 81-103, 1990.

Bibring, J.-P., Y. Langevin, A. Gendrin, B. Gondet, F. Poulet, M. Berthé, A. Soufflot, R. Arvidson, N. Mangold, J. Mustard, P. Drossart, and the OMEGA team, Mars Surface Diversity as Revealed by the OMEGA/Mars Express Observations. *Science 307*, 1576-1581, 2005.

Bigham, J. M., and D. K. Nordstrom, Iron and aluminum hydroxysulfates from acid sulfate waters, In C. N. Alpers, J. L. Jambor, and D. K. Nordstom, Sulfate minerals: Crystallography, geochemistry, and environmental significance. *Rev. Mineral. Geochem., Mineral. Soc. Amer. & Geochem. Soc., Vol. 40,* pp. 351-403, 2000.

Boyd, F. R., and S. A. Mertzman, Composition and structure of the Kaapvaal lithosphere, southern Africa, In: Mysen, B.O. (ed.), Magmatic Processes - Physicochemical Principles. The Geochemical Society, Special Publication No. 1, pp. 13-24, 1987.

Burns, R.G., Gossans on Mars. Proc. Lunar Planet. Sci XVIII, pp. 713-721, 1988.

Burns, R. G., and D. S. Fisher, Iron-sulfur mineralogy of Mars: Magmatic evolution and chemical weathering products, *J. Geophys. Res., 95,* 14169-14173, 1990.

Clark, B.C. and A.K. Baird, Is the Martian lithosphere sulfur rich? *J. Geophys. Res., 84,* 8395-8503, 1979.

Clark, B.C., A. K. Baird, R. J. Weldon, D. M. Tsusaki, L. Schnabel, and M. P. Candelaria, Chemical composition of Martian fines, *J. Geophys. Res., 87,* 10,059-10,067, 1982.

Clark, B.C., R. V. Morris, S. M. McLennan, R. Gellert, B. Jolliff, A. H. Knoll, S. W. Squyres, T. K. Lowenstein, D. W. Ming, N. J. Tosca, A. Yen, P. R. Christensen, S. Gorevan, J. Brückner, W. Calvin, G. Dreibus, W. Farrand, G. Klingelhoefer, H. Waenke, J. Zipfel, J. F. Bell III, J. Grotzinger, H. Y. McSween, and R. Rieder, Chemistry and mineralogy of outcrops at Meridiani Planum, *Earth Planet. Sci. Lett.*, (2005, submitted).

Fernández-Remolar, D.C., R. V. Morris, J. E. Gruener, R. Amils, and A. H. Knoll, The Rio Tinto Basin Spain, Mineralogy, sedimentary geobiology, and implications for interpretation of outcrop rocks at Meridiani Planum, Mars, *Earth Planet. Sci. Lett.*, (2005, submitted).

Gellert, R., R. Rieder, R. C. Anderson, J. Brückner, B. C. Clark, G. Dreibus, T. Economou, G. Klingelhöfer, G. W. Lugmair, D. W. Ming, S. W. Squyres, C. d'Uston, H. Wänke, A. Yen, J. Zipfel, Chemical composition of Martian rocks and soils at the Spirit landing site in Gusev crater: Initial results of the Alpha Particle X-ray Spectrometer, *Science, 305,* 829-832, 2004.

Gendrin, A., N. Mangold, J.-P. Bibring, Y. Langevin, B. Gondet, F. Poulet, G. Bonello, C. Quantin, J. Mustard, R. Arvidson, and S. LeMouélic, Sulfates in Martian Layered Terrains: The OMEGA/Mars Express View, *Science, 307,* 1587-1591, 2005.

Golombek, M. P., J .A. Grant, T. J. Parker, D. M. Kass, J. A. Crisp, S. W. Squyres, A. F. C. Haldemann, M. Alder, N. T. Bridges, R. E. Arvidson, M. H. Carr, R. L. Kirk, P. C. Knocke, R. B. Roncoli, C. M. Weitz, J. T. Schofield, R. W. Zurek, P. R. Christensen, R. L. Fergason, F. S. Anderson, and J. W. Rice, Jr, Selection of the Mars Exploration Rover landing sites, *J. Geophys. Res., 108*(E12), doi:10.1029/2002JE002074, 2003.

Grandstaff, D.E. The dissolution rate of forsteritic olivine from Hawaiian beach sand. In: S. M. Colman, D. P. Dethier (eds.), Rates of chemical weathering of rocks and minerals. New York: Academic Press, p. 41-59, 1986.

Haskin, L. A., A. Wang, B. L. Jolliff, H. Y. McSween, B. C. Clark, D. J. Des Marais, S. M. McLennan, N. J. Tosca, J. A. Hurowitz, J. D. Farmer, A.Yen, S. W. Squyres, R. E. Arvidson, G. Klingelhöfer, C. Schröder, P. de Souza, D. W. Ming, R. Gellert, J. Zipfel, J. Brückner, J. F. Bell, III, K. Herkenhoff, P. R. Christensen, S. Ruff, D. Blaney, S. Gorevan,

N. A. Cabrol, L. Crumpler, J. Grant, and L. Soderblom, Water alteration of rocks and soils from the Spirit rover site, Gusev crater, Mars, *Nature*, 436, 66-69.

Herkenhoff, K.E., S. W. Squyres, R. Arvidson, D. S. Bass, J. F. Bell, III, P. Bertelsen, B. L. Ehlmann, W. Farrand, L. Gaddis, R. Greeley, J. Grotzinger, A. G. Hayes, S. F. Hviid, J. R. Johnson, B. Jolliff, K. M. Kinch, A. H. Knoll, M. B. Madsen, J. N. Maki, S. M. McLennan, H. Y. McSween, D. W. Ming, J. W. Rice, Jr., L. Richter, M. Sims, P. H. Smith, L. A. Soderblom, N. Spanovich, R. Sullivan, S. Thompson, T. Wdowiak, C. Weitz, and P. Whelley, Evidence from Opportunity's Microscopic Imager for Water on Meridiani Planum, Science, *306,* 1727-1730, 2004

Klingelhöfer, G., R. V. Morris, B. Bernhardt, C. Schröder, D. S. Rodionov, P.A. de Souza, Jr., A. Yen, R. Gellert, E. N. Evlanov, B. Zubkov, J. Foh, U. Bonnes, E. Kankeleit, P. Gütlich, D. W. Ming, F. Renz, T. Wdowiak, S. W. Squyres, R. E. Arvidson, Jarosite and hematite at Meridiani Planum from the Mössbauer Spectrometer on the Opportunity Rover, *Science 306,* 1740-1745, 2004.

Langevin, Y., F. Poulet, J-.P. Bibring, J.-P., and B. Gondet, Sulfates in the North Polar region of Mars detected by OMEGA/Mars Express, *Science, 307,* 1584-1586, 2005.

McLennan, S. M., J. F. Bell III, W. M. Calvin, P. R. Christensen, B. C. Clark, P. A. de Souza, J. Farmer, W. H. Farrand, D. Fike, R. Gellert, A. Ghosh, T. D. Glotch, J. P. Grotzinger, B. Hahn, K. E. Herkenhoff, J. A. Hurowitz, J. R. Johnson, S. S. Johnson, B. Jolliff, G. Klingelhöfer, A. H. Knoll, Z. Learner, M. C. Malin, H. Y. McSween Jr,. J. Pocock, S. W. Ruff, L. A. Soderblom, S. W. Squyres, N. J. Tosca, W. Watters, M. B. Wyatt, and A. Yen, Provenance and diagenesis of the Burns formation, Meridiani Planum, Mars, *Earth Planet. Sci. Lett.*, (2005, submitted).

McSween, H. Y., R. E. Arvidson, J. F. Bell III, D. Blaney, N. A. Cabrol, P. R. Christensen, B. C. Clark, J. A. Crisp, L. S. Crumpler, D. J. Des Marais, J. D. Farmer, R. Gellert, A. Ghosh, S. Gorevan, T. Graff, J. Grant, L. A. Haskin, K. E. Herkenhoff, J. R. Johnson, B. L. Jolliff, G. Klingelhoefer, A. T. Knudson, S. McLennan, K. A. Milam, J. E. Moersch, R. V. Morris, R. Rieder, S. W. Ruff, P. A. de Souza, Jr., S. W. Squyres, H. Wänke, A. Wang, M. B. Wyatt, A. Yen, and J. Zipfel, Basaltic rocks analyzed by the Spirit Rover in Gusev crater, *Science, 305*, 842-845, 2004.

Ming, D. W., D. W. Mittlefehldt, R. V. Morris, D. C. Golden, R. Gellert, A. Yen, B. C. Clark, S. W. Squyres, W. H. Farrand, S. W. Ruff, R. A. Arvidson, G. Klingelhöfer, H. Y. McSween, D. S. Rodionov, C. Schröder, P. A. de Souza, Jr., and A. Wang. Geochemical and mineralogical indicators for aqueous processes in the Columbia Hills of Gusev crater, Mars. *J. Geophy. Res.*, (2005b, in review).

Ming, D. W., R. V. Morris, R. Gellert, A. Yen, J. F. Bell, III, D. Blaney, P. R. Christensen, L. Crumpler, P. Chu, W. H. Farrand, S. Gorevan, K. E. Herkenhoff, G. Klingelhöfer, R. Rieder, D. S. Rodionov, S. W. Ruff, C. Schröder, S. W. Squyres, and the Athena Science Team, Geochemical and mineralogical indicators for aqueous processes on the West Spur of the Columbia Hills in Gusev crater, in *Lunar Planet. Sci. XXXVI*, Lunar and Planetary Institute, Houston, Texas (CD-ROM), Abstract #2125, 2005a.

Moore, H. J., R. M. Hutton, G. D. Clow, and C. R. Spitzer, Physical properties of surface materials at the Viking landing sites on Mars, *U.S.G.S. Prof. Paper 1389*, 1987.

Moore, H. J., Liebes, Jr., D. S. Crouch, L. V. Clark, Rock pushing and sampling under rocks on Mars, U.S.G.S. Prof. Paper 1081, 1978.

Morris, R. V., D. G. Agresti, H. V. Lauer Jr., J. A. Newcomb, T. D. Shelfer, and A. V. Murali, Evidence for pigmentary hematite on Mars based on optical, magnetic, and Mossbauer studies of superparamagnetic (nanocrystalline) hematite, *J. Geophys. Res., 94*, 2760-2778, 1989.

Morris, R. V., D. C. Golden, J. F. Bell, III, T. D. Shelfer, A. C. Scheinost, N. W. Hinman, G. Furniss, S. A. Mertzman, J. L. Bishop, D. W. Ming, C. C. Allen, and D. T. Britt, Mineralogy, composition, and alteration of Mars Pathfinder rocks and soils: Evidence from multispectral, elemental, and magnetic data on terrestrial analogue, SNC meteorite, and Pathfinder samples, *J. Geophys. Res.-Planets, 105*, 1757-1817, 2000.

Morris, R. V., G. Klingelhöfer, B. Bernhardt, C. Schröder, D. S. Rodionov, P. A. de Souza Jr., A. Yen, R. Gellert, E. N. Evlanov, D. W. Ming, F. Renz, T. Wdowiak, S. W. Squyres, R. E. Arvidson, and the Athena Science Team, Mössbauer mineralogy on Mars: First results from the Spirit landing site in Gusev crater, *Science, 305*, 833-836, 2004.

Morris, R. V., H. V. Lauer Jr., C. A. Lawson, E. K. Gibson Jr., G. A. Nace, and C. Stewart, Spectral and other physicochemical properties of submicron powders of hematite (a-Fe_2O_3), maghemite (g-Fe_2O_3), magnetite (Fe_3O_4), goethite (a-FeOOH), and lepidocrocite (g-

FeOOH), *J. Geophys. Res., 90,* 3126-3144, 1985.

Morris, R. V., D. W. Ming, B. C. Clark, G. Klingelhoefer, R. Gellert, D. Rodionov, C. Schroeder, P. de Souza, A. Yen, and the Athena Science Team, Abundance and speciation of water and sulfate at Gusev crater and Meridiani Planum, In *Lunar and Planetary Science XXXVI*, Abstract #2239, Lunar and Planetary Institute, Houston (CD-ROM), 2005.

Morris, R. V., D. W. Ming, D. C. Golden, and J. F. Bell, III, An occurrence of jarositic tephra on Mauna Kea, Hawaii: Implications for the ferric mineralogy of the martian surface. In: M. D. Dyer, C. McCammon, and M. W. Schaefer, (eds.), Mineral Spectroscopy: A Tribute to Roger G. Burns, Special Publication No. 5, The Geochemical Society, Houston, Texas, pp. 327-336, 1996.

Rieder, R., R. Gellert, R. C. Anderson, J. Brückner, B. C. Clark, G. Dreibus, T. Economou, G. Klingelhöfer, G. W. Lugmair, D. W. Ming, S. W. Squyres, D. d'Uston, H. Wänke, A. Yen, and J. Zipfel, Chemistry of Rocks and Soils at Meridiani Planum from the Alpha Particle X-ray Spectrometer, *Science,* 306, 1746-1749, 2004.

Squyres, S. W., R. Arvidson, J. F. Bell III, J. Brückner, N. A. Cabrol, W. Calvin, M. H. Carr, P. R. Christensen, B. C. Clark, L. Crumpler, D. J. Des Marais, C. d'Uston, J. Farmer, W. Farrand, W. Folkner, M. Golombek, S. Gorevan, J. A. Grant, R. Greeley, J. Grotzinger, L. Haskin, K. E. Herkenhoff, S. Hviid, J. Johnson, A. Knoll, G. Landis, M. Lemmon, R. Li, M. B. Madsen, M. C. Malin, S. McLennan, H. Y. McSween, D. W. Ming, J. Moersch, R. V. Morris, T. Parker, J. W. Rice Jr., L. Richter, R. Rieder, M. Sims, M. Smith, P. Smith, L. A. Soderblom, R. Sullivan, H. Wänke, T. Wdowiak, M. Wolff, and A. Yen, Initial results from the Athena Science Investigation at Gusev crater, Mars, *Science, 305*, 794-799, 2004a.

Squyres, S. W., J. P. Grotzinger, R. E. Arvidson, J. F. Bell III, P. R. Christensen, B. C. Clark, J. A. Crisp, W. H. Farrand, K. E. Herkenhoff, J. R. Johnson, G. Klingelhöfer, A. H. Knoll, S. M. McLennan, H. Y. McSween Jr., R. V. Morris, J. W. Rice Jr., R. Rieder, and L. A. Soderblom, In situ evidence for an ancient aqueous environment on Mars, *Science, 306* 1709-1714, 2004b.

Tosca, N. J., S. M. McLennan, B. C. Clark, J. P. Grotzinger, J. A. Hurowitz, A. H. Knoll, C. Schröder, and S. W. Squyres, Geochemical modeling of evaporation processes on Mars: Insight from the sedimentary record at Meridiani Planum, *Earth Planet. Sci. Lett.*, (2005, submitted).

Tosca, N. J., S. M. McLennan, D. H. Lindsley and M. A. A. Schoonen, Acid-sulfate weathering of synthetic Martian basalt: The acid fog model revisited, *J. Geophys. Res.*, *109*(E05003), doi:10.1029/2003JE002218, 2004.

Van Breeman, N, Acid sulfate soils, In Land Reclamation and Water Management, ILRI Publ. 27, Waganingan, The Netherlands, p. 53-57, 1980.

Vaniman, D. T., S. J. Chipera, D. L. Bish, J. W. Carey, and W. C. Feldman, Martian relevance of dehydration and rehydration in the Mg-sulfate system, In *Lunar and Planetary Science XXXVI*, Abstract #1486, Lunar and Planetary Institute, Houston (CD-ROM), 2005.

Wogelius R. A., and J. V. Walther, Olivine dissolution kinetics at near-surface conditions, *Chem. Geol.*, *97*, 101-112, 1992

Yen, A. S., R. Gellert, C. Schröder, J. F. Bell III, R. V. Morris, A. T. Knudson, B. C. Clark, D. W. Ming, J. A. Crisp, R. E. Arvidson, D. Blaney, J. Brückner, P. Christensen, D. J. DesMarais, P. de Souza, T. Economou, A. Ghosh, B. Hahn, K. E. Herkenhoff, L. A. Haskin, J. A. Hurowitz, B. L. Joliff, J. R. Johnson, G. Klingelhöfer, M. B. Madsen, S. M. McLennan, H. Y. McSween, L. Richter, R. Rieder, D. Rodionov, L. Soderblom, S. W. Squyres, N. J. Tosca, A. Wang, M. Wyatt, and J. Zipfel, An integrated view of the chemistry and mineralogy of Martian soils, *Nature*, 425, 49-54, 2005.

Zent, A. P., and C. P. McKay, The chemical reactivity of the Martian soil and implications for future missions, *Icarus*, *108*, 146-157, 1994.

Figure Captions

Figure 1. Secondary electron backscatter images of epoxy imbedded sectioned HWPC100 grains: a) general view of particles containing olivine, pyroxene (px), and plagioclase feldspar in a glass matrix, and b) plagioclase feldspar (pf) and olivine (ol) in a glass matrix.

Figure 2. Secondary electron backscattered images of epoxy imbedded sectioned HWMK725 grains: a) general view of particles containing plagioclase feldspars, olivine and titanomagnetite in the glass matrix, b) plagioclase feldspar (pl) and olivine (ol) grains in the matrix of glass (gl), and c) titanomagnetite (tm).

Figure 3. X-ray diffraction patterns of untreated and acid fog treated HWPC100 basaltic sand grains (0.5-1.0 mm). The untreated sample consists mostly of olivine (ol) and a trace of titanomagnetite and pyroxene. No additional phases were identified in the acid fog treated samples at time zero. Hexahydrite (hx) was the only phase to form in treated samples after exposure to 54% RH conditions for 72 hours.

Figure 4. SEM secondary electron images of sulfuric acid vapor treated olivine rich HWPC100 basalt sample exposed to 56% RH for 72 hours. (a) A large gypsum (gy) crystal (approx. 20 μm across) has formed on the surface of a plagioclase feldspar crystal. (b) Small Ca sulfate crystals (light-toned crystals) have formed on the surface of a plagioclase feldspar (pf) crystal. The plagioclase feldspar has been etched by the sulfuric acid vapor treatment. (c) Mg sulfate (ms) crystals have formed near the interface of a particle and epoxy that suggests the mobility of Mg to this interface and the subsequent precipitation of the Mg sulfate. (d) Mg sulfate (ms) crystals and amorphous silica have completely replaced an olivine crystal. The surround glass (gl) appears to have experience little alteration at the surface as suggested by the lack of precipitates.

Figure 5. X-ray diffraction patterns for air-dried residues of three-step and single-step leaching experiments of olivine-rich basalt sample HWPC100 (0.5-1.0 mm). The untreated pattern is for the original HWPC100 starting material prior to sulfuric acid treatment, OS-1 is the residue after the first “leaching” treatment in the three-step leaching experiment, OS-2 is the residue after the second “leaching” treatment in the three-

step leaching experiment, OS-3 is the residue after the third and final "leaching" treatment in the three-step leaching experiment, and CS is the residue after treatment in the single-step batch experiment [ol = olivine; gy = gypsum; hx = hexahydrite; j = jarosite, pf = plagioclase feldspar, px = pyroxene].

Figure 6. SEM secondary electron images of olivine-rich basaltic sand HWPC100 (<53μm) prior to and after treatment in the single-step and three-step leaching experiments. (a) Untreated sample illustrating the shape and texture of unaltered glass (gl) shards along with finer materials. (b) Residue after single-step batch experiment that illustrates a leached surface (ls) of a glass shard and the formation of amorphous silica (as) on the surface of the shard. (c) A large gypsum crystal and small Mg sulfate crystals have formed after the third leaching step of the three-step leaching experiment. These phases likely formed from evaporation of solutions remaining adsorbed to particles after solutions were decanted and separated from the residue. (d) Jarosite (j) crystals that have formed after the third leaching step in the three-step leaching experiment. These crystals are composed of Fe and S with minor amounts of Na. The lack of K and minor Na suggests that the variety of jarosite that formed in the open system was hydronium jarosite.

Figure 7. Mössbauer spectra (293 K) for olivine-rich basaltic sand HWPC100 (0.5-1.0 mm) prior to and after sulfuric acid treatment in the three-step leaching experiment. The spectrum of the untreated sample was dominated by glass and olivine. Jarosite and glass were the dominant phases in the MB spectrum after sulfuric acid treatment. A natural jarosite-rich tephra sample from near the summit of Mauna Kea Volcano in Hawaii has a very similar MB spectrum when compared to the sulfuric acid treated HWPC100.

Figure 8. X-ray diffraction patterns of untreated and acid fog treated HWMK725 basaltic tephra grains (0.5-1.0 mm). The untreated sample is mostly plagioclase feldspar (pf). The treated sample X-rayed at time zero (i.e., immediately at completion of experiment) had a few additional peaks that were probably due to transient phases (T_1-T_4) aluminum hydrogen sulfate and an anhydrous ferric sulfate. Alunogen (al), hexahydrite (hx), and voltaite (vo) were the primary sulfates that formed after exposing the acid fog treated samples to 56% RH conditions for 72 hours.

Figure 9. SEM secondary electron images of sulfuric acid vapor treated plagioclase feldspar-rich HWMK725 basalt samples exposed to 56% RH for 72 hours. (a) Platy alunogen (al) crystals formed at the interface of the basaltic tephra grain and epoxy (ep). Olivine (dark crystals) and plagioclase feldspar laths are in a matrix of glass (gl). Ca sulfate crystals decorate the surface of the grain. (b) Amorphous silica (as) has completely replaced olivine crystals (dark crystal casts). Elongated rod-shaped crystals near the top of this image are gypsum (gy). The surfaces of the glass (gl) and replaced olivine crystals are decorated with Ca sulfate crystals. (c) Small white Ca sulfate crystals decorate the surfaces of plagioclase feldspar (pl) and glass (gl) and alunogen (al) plates have formed near the edge of the particle. (d) Ca sulfate crystals decorate the surface of glass that was initially rich in Ca. An olivine cast (dark area not decorated with Ca sulfate crystals) has been replaced by amorphous silica (as).

Figure 10. X-ray diffraction patterns for air-dried residues of the three-step and single-step batch experiments for 0.5-1.0 mm plagioclase feldspar-rich basalt sample HWMK725. The untreated pattern is for the original HWPC100 starting material prior to sulfuric acid treatment, OS-1 is the residue after the first "leaching" treatment in the three-step leaching experiment, OS-2 is the residue after the second "leaching" treatment in the three-step leaching experiment, OS-3 is the residue after the third and final "leaching" treatment in the three-step leaching experiment, and CS is the residue after treatment in the single-step batch experiment. All peaks in this sample are for plagioclase feldspar. A very broad peak (18-32 $^{o}2\theta$) is assigned to amorphous silica.

Figure 11. Solution chemistry of leachates for basaltic samples HWMK725 and HWPC100 after sulfuric acid treatments in the three-step and single-step batch experiments [OS-1, OS-2, OS-3 = leachate after first, second, and third "leaching" steps, respectively, in the three-step leaching experiment; CS = leachate after sulfuric acid treatment in the single-step batch experiment]. (a) Elemental concentrations for plagioclase feldspar-rich basaltic tephra HWMK725 (0.5-1.0 mm). (b) Elemental concentrations for olivine-rich basaltic sand HWPC100 (0.5-1.0 mm) (c) Solution pH for

plagioclase feldspar-rich basaltic tephra HWMK725 (0.5-1.0 mm). (d) Solution pH for olivine-rich basaltic sand HWPC100 (0.5-1.0 mm).

Supplemental Figures

Supplemental Figure 1: Hydrated magnesium sulfate minerals (ms) on the sulfuric acid vapor exposed HWPC100 olivine-rich basalt. An energy dispersive spectrum (EDS) of the spheroidal crystals show the high Mg and S compositions that indicate these are magnesium sulfate crystals. The EDS peak close to 0 kV is due to C coating.

Supplemental Figure 2: X-ray diffraction patterns for air-dried residues of three-step and single-step leaching experiments of olivine-rich basalt sample HWPC100 (< 53 μm starting materials). The untreated pattern is for the original HWPC100 starting material prior to sulfuric acid treatment, OS-1 is the residue after the first "leaching" treatment in the three-step leaching experiment, OS-2 is the residue after the second "leaching" treatment in the three-step leaching experiment, OS-3 is the residue after the third and final "leaching" treatment in the three-step leaching experiment, and CS is the residue after treatment in the single-step batch experiment [ah = anhydrite; ba = bassanite; gy = gypsum; j = jarosite, pf = plagioclase feldspar]. Plagioclase feldspar is present in all samples as a residue inherited from the parent basalt. The broad hump in the 18-32 degrees 2-theta range is due to amorphous silica.

Tables

Table 1. Bulk composition of basaltic starting materials for sulfuric acid weathering experiments.

Oxide	HWPC100[a]	HWMK725[b]
	wt. %	
SiO_2	46.09	51.62
TiO_2	1.81	2.32
Al_2O_3	9.29	17.86
Fe_2O_3T[c]	14.89	11.47
MnO	0.20	0.23
MgO	17.73	3.06
CaO	7.52	6.07
Na_2O	1.54	4.38
K_2O	0.32	1.91
P_2O_5	0.18	1.03
Total	99.95	100.16
% LOI	0.95	3.80
FeO	11.55	5.35
Fe_2O_3	2.05	5.53
$Fe^{3+}/Fe_{(Total)}$	0.14	0.48
Cl	0.132	0.00

[a]Basaltic sand, Kalpana, Puna Coast, Island of Hawaii.
[b]Basaltic tephra, Mauna Kea volcano, Island of Hawaii.
[c]Total Fe as Fe_2O_3.

Table 2. Secondary weathering products and remaining residual phases after exposing two basaltic materials to simulated sulfuric acid weathering conditions.

Acid-Sulfate Simulated Environment	(particle size)	XRD Analysis Immediately after experiment ended		XRD Analysis After 72 h exposure to 54% RH		SEM/EDS Analyses* After 72 h exposure to 54% RH	
		HWPC100	HWMK725	HWPC100	HWMK725	HWPC100	HWMK725
Acid Fog, Natural particles		olivine, plag. feldspar	$AlH(SO_4)_2$, $Fe_2(SO_4)_3$, amorph. silica, plag. feldspar	hexahydrite, olivine, plag. feldspar	alunogen, hexahydrite, voltaite, amorph. silica, plag. feldspar	$MgSO_4.nH_2O$, amorph. silica	alunogen, halite, amorph. silica
Acid Fog, Thin sections		NA	NA	NA	NA	$MgSO_4 \cdot nH_2O$,amorph. silica, Ca-sulfate, gypsum, minor alunogen	alunogen, Ca-sulfate, gypsum, amorph. silica
Three-Step Leaching Experiments	0.5-1.0 mm	jarosite, gypsum, amorph. Silica, plag. Feldspar, pyroxene	plag. feldspar	NA	NA	jarosite, gypsum, amorph. silica, $MgSO_4 \cdot nH_2O$	amorph. silica
	<53 μm	jarosite, anhydrite, gypsum, amorph. silica, plag. Feldspar, pyroxene	amorph. silica, plag. feldspar	NA	NA	jarosite, gypsum, amorph. silica, $MgSO_4 \cdot nH_2O$	amorph. silica
Single-Step Batch Experiments	0.5-1.0 mm and <53 μm	amorph. silica, plag. Feldspar, pyroxene	amorph. silica, plag. feldspar	NA	NA	amorph. silica	amorph. silica

*Primary phases (plag. feldspar, olivine, pyroxene) are not listed for SEM/EDS analysis.
NA = Not Applicable. Experiments were not conducted.

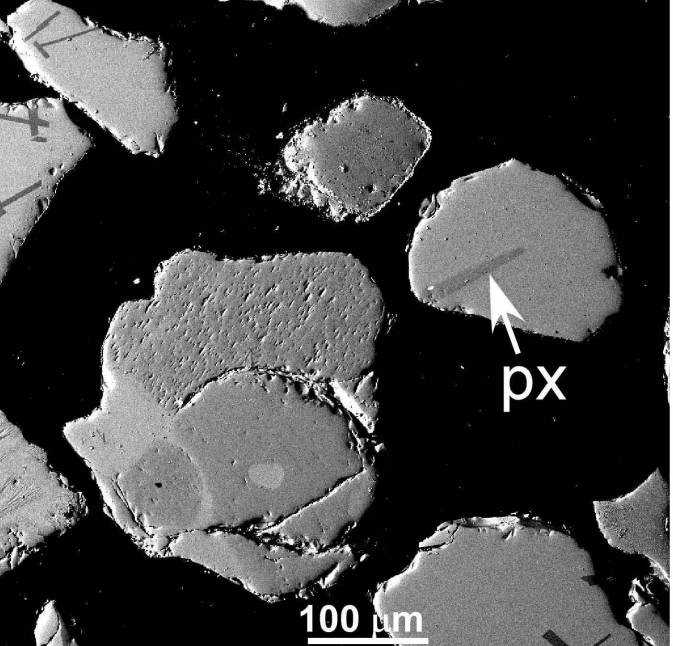
px
100 µm

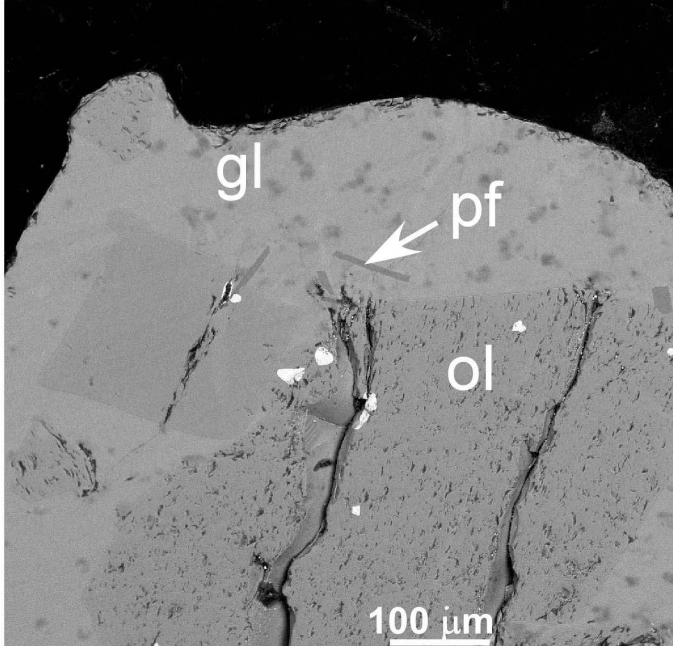
gl
pf
ol
100 µm

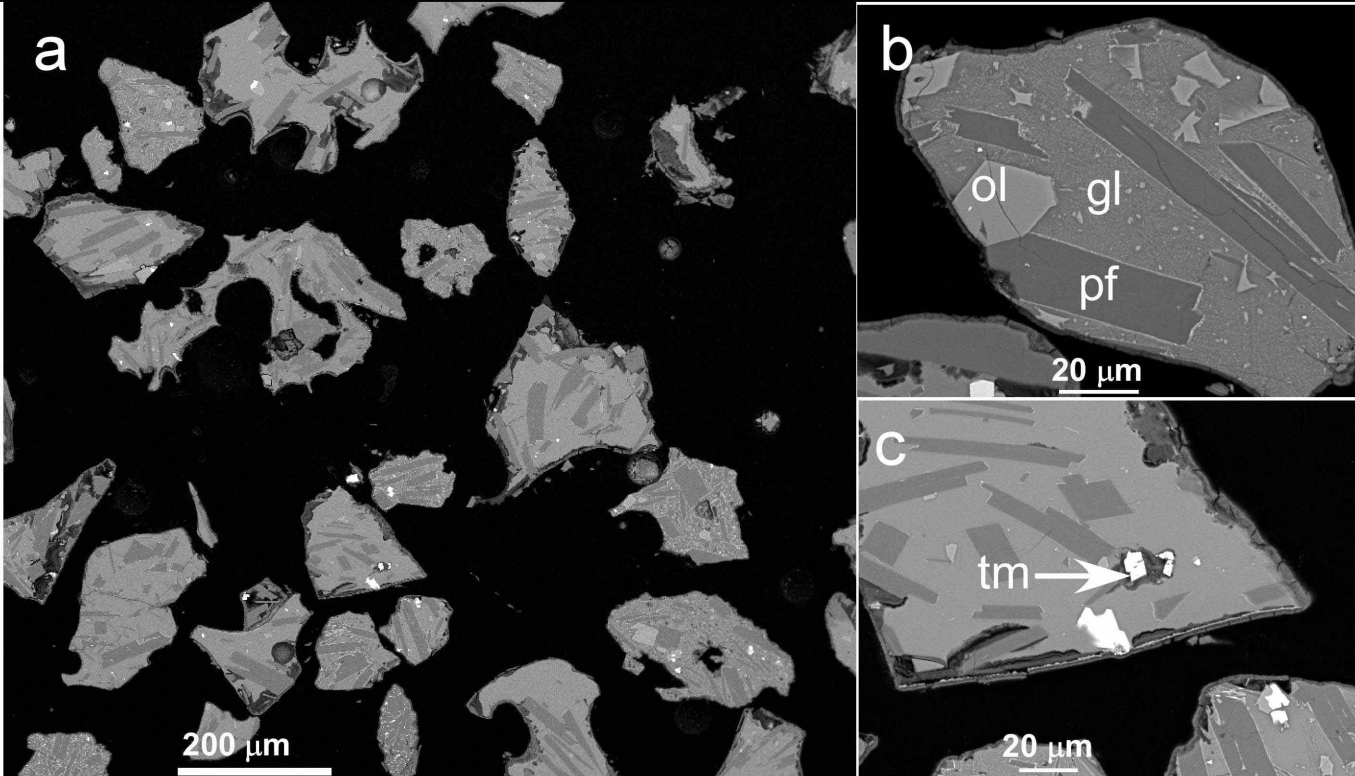
a
200 μm
b
ol
gl
pf
20 μm
c
tm
20 μm

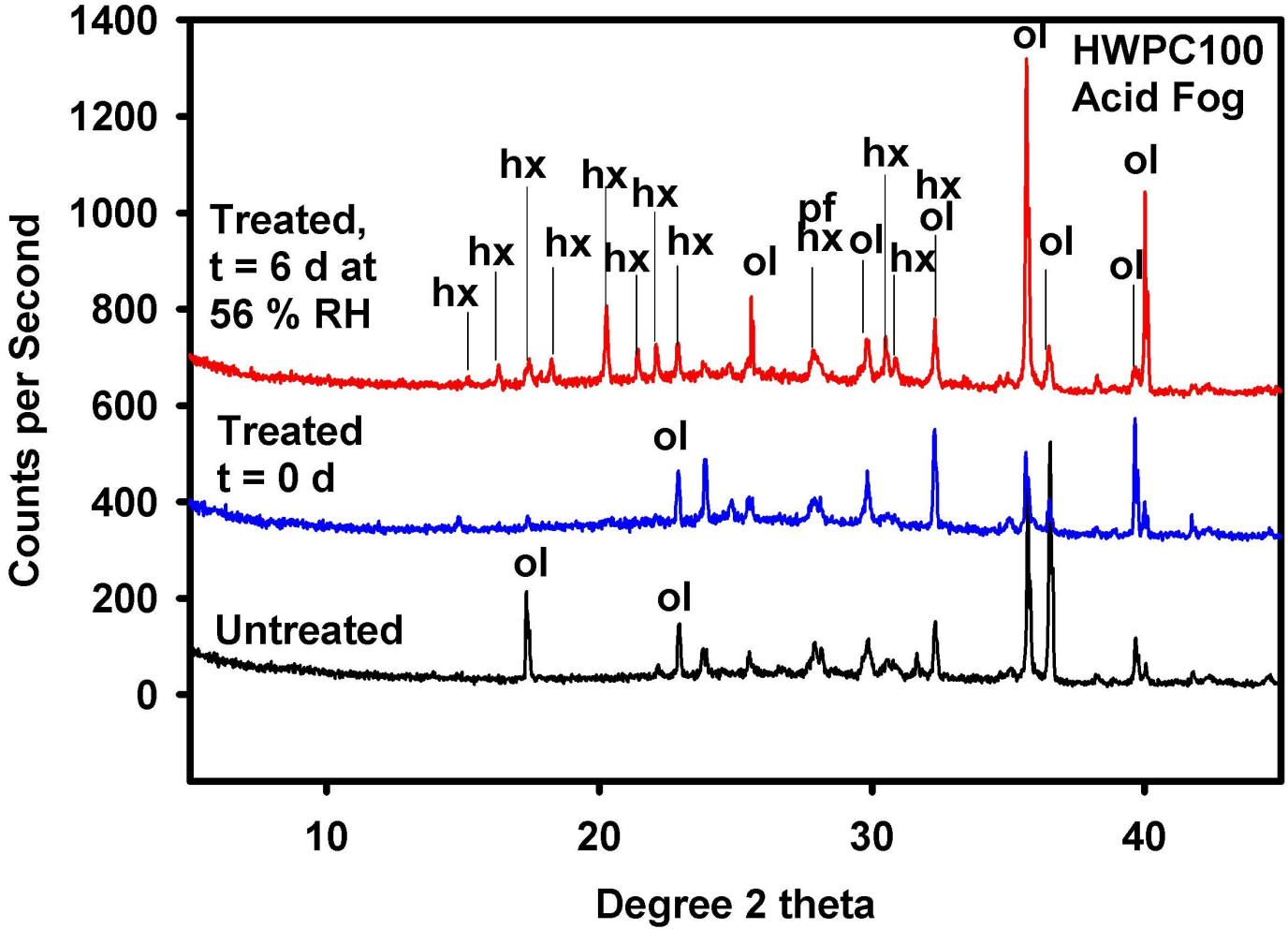
HWPC100
Acid Fog
Treated,
t = 6 d at
56 % RH
Treated
t = 0 d
Untreated
hx
ol
pf
Counts per Second
Degree 2 theta
0
200
400
600
800
1000
1200
1400
10
20
30
40

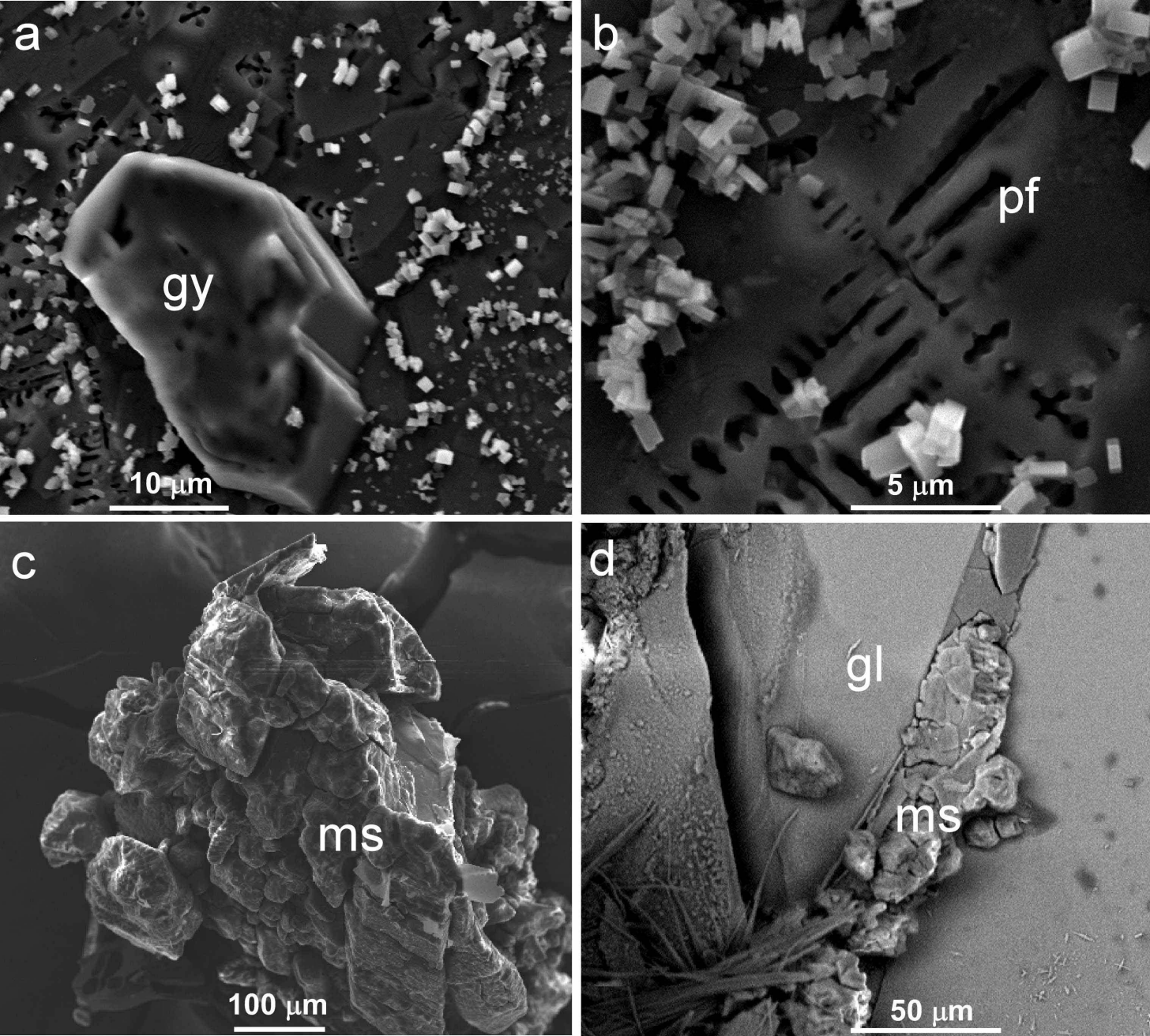
a
gy
10 μm
b
pf
5 μm
c
ms
100 μm
d
gl
ms
50 μm

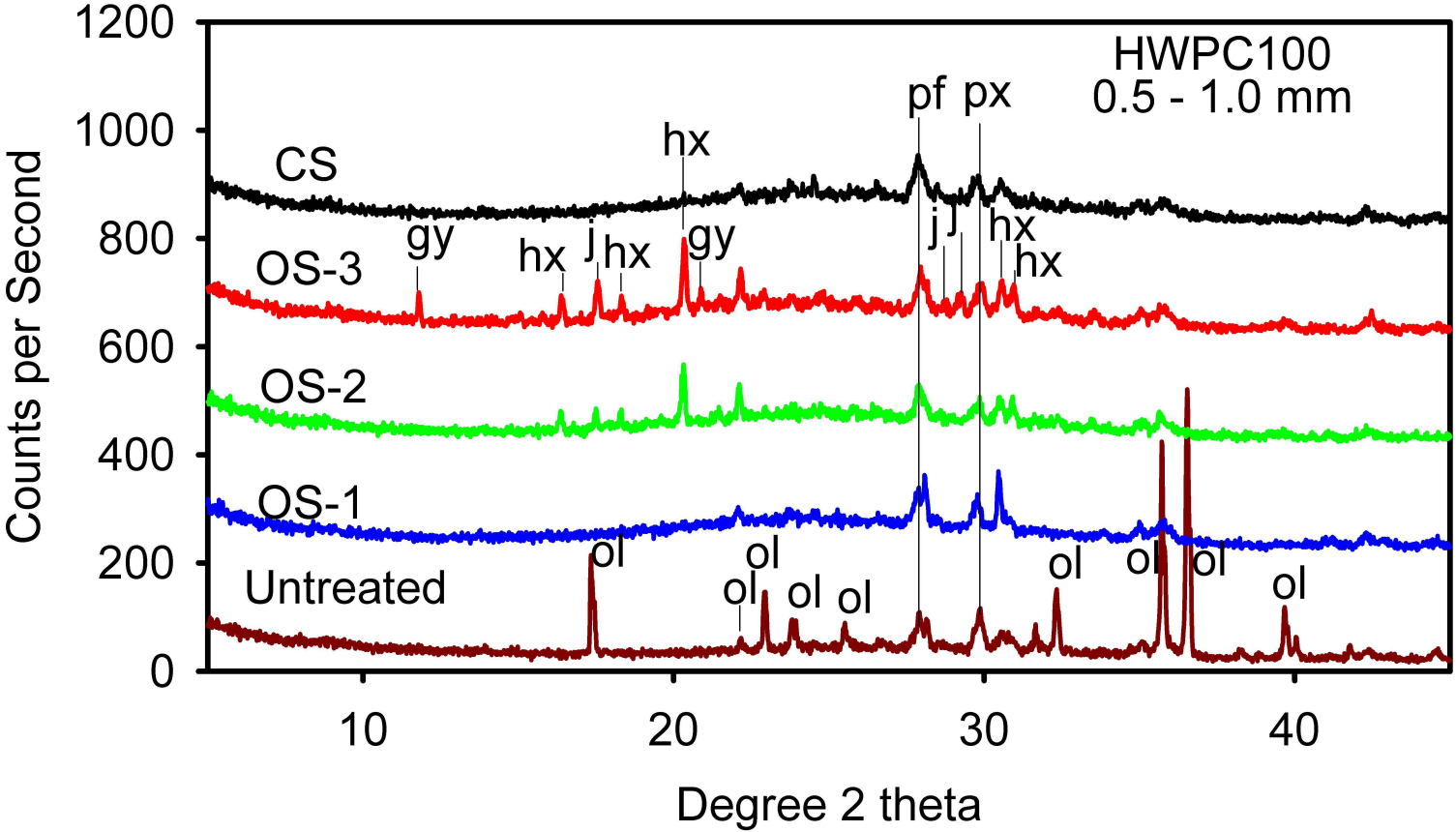
HWPC100
0.5 - 1.0 mm
CS
OS-3
OS-2
OS-1
Untreated
pf
px
hx
gy
j
ol
Counts per Second
Degree 2 theta
0
200
400
600
800
1000
1200
10
20
30
40

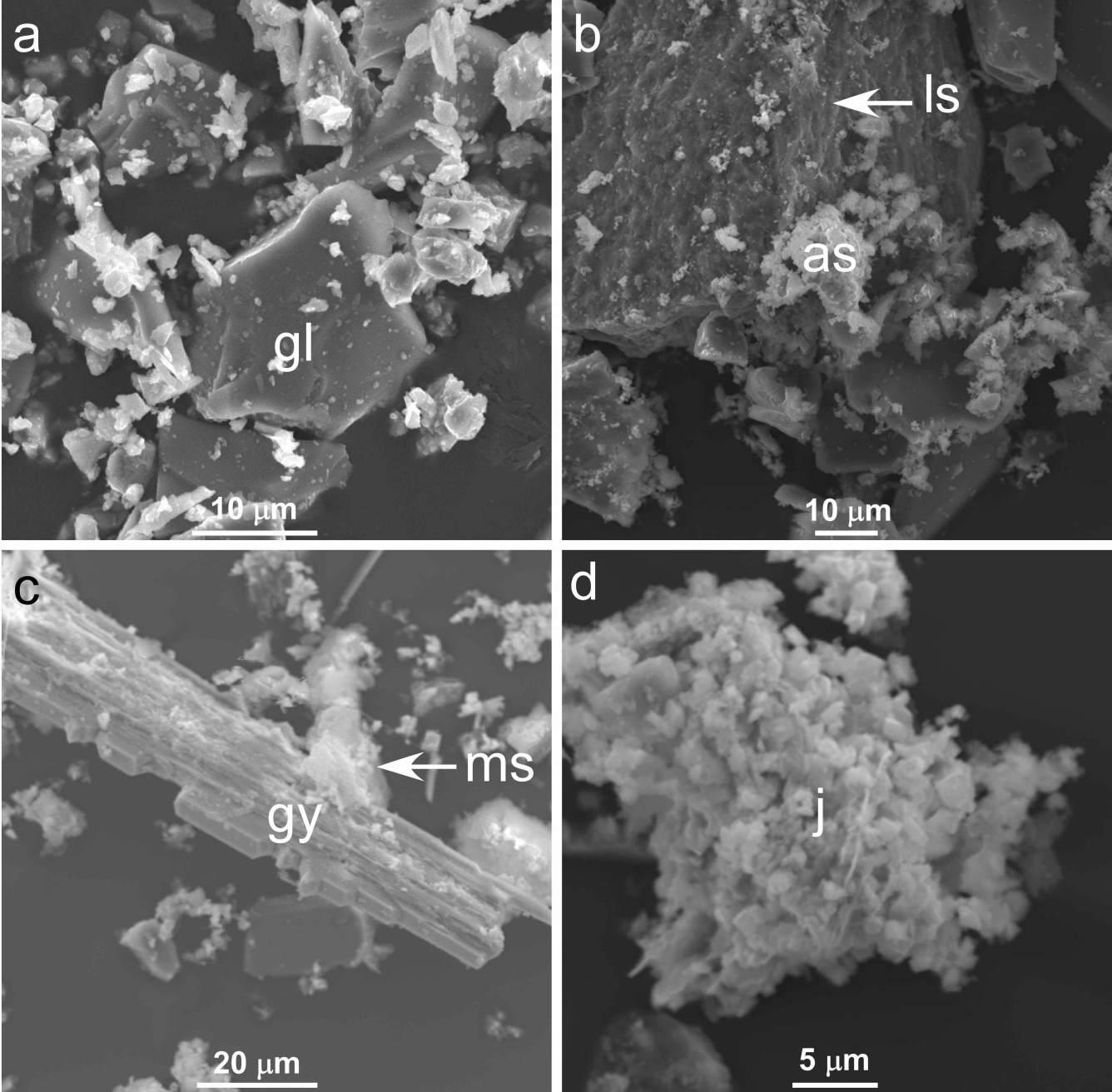
a
gl
10 μm
b
ls
as
10 μm
c
ms
gy
20 μm
d
j
5 μm

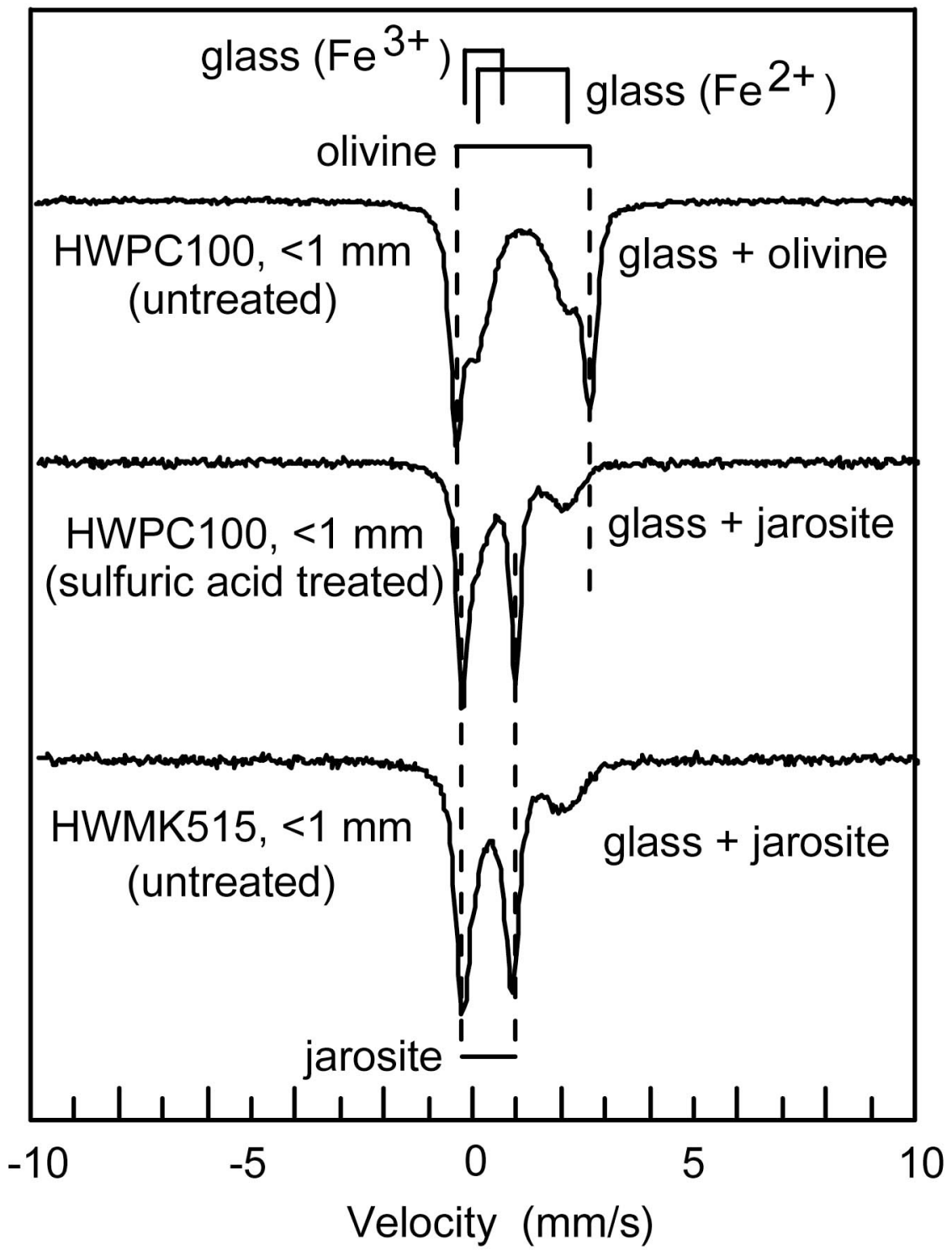
glass (Fe 3+)
glass (Fe 2+)
olivine
HWPC100, <1 mm
(untreated)
glass + olivine
HWPC100, <1 mm
(sulfuric acid treated)
glass + jarosite
HWMK515, <1 mm
(untreated)
glass + jarosite
jarosite
-10
-5
0
5
10
Velocity (mm/s)

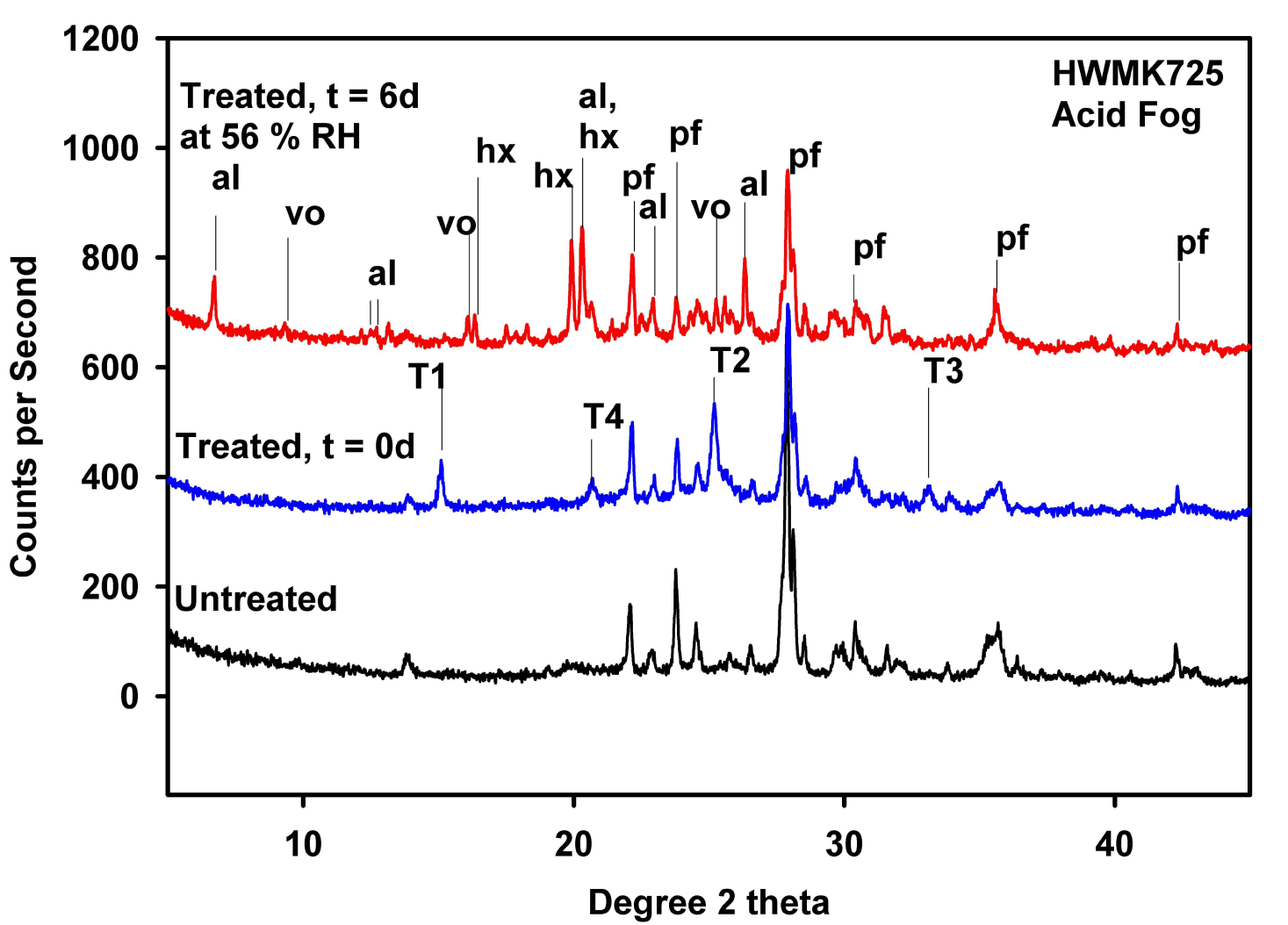
HWMK725
Acid Fog
Treated, t = 6d
at 56 % RH
Treated, t = 0d
Untreated
al
vo
al
vo
hx
hx
al,
hx
pf
al
pf
vo
al
pf
pf
pf
pf
T1
T4
T2
T3
Counts per Second
Degree 2 theta
0
200
400
600
800
1000
1200
10
20
30
40

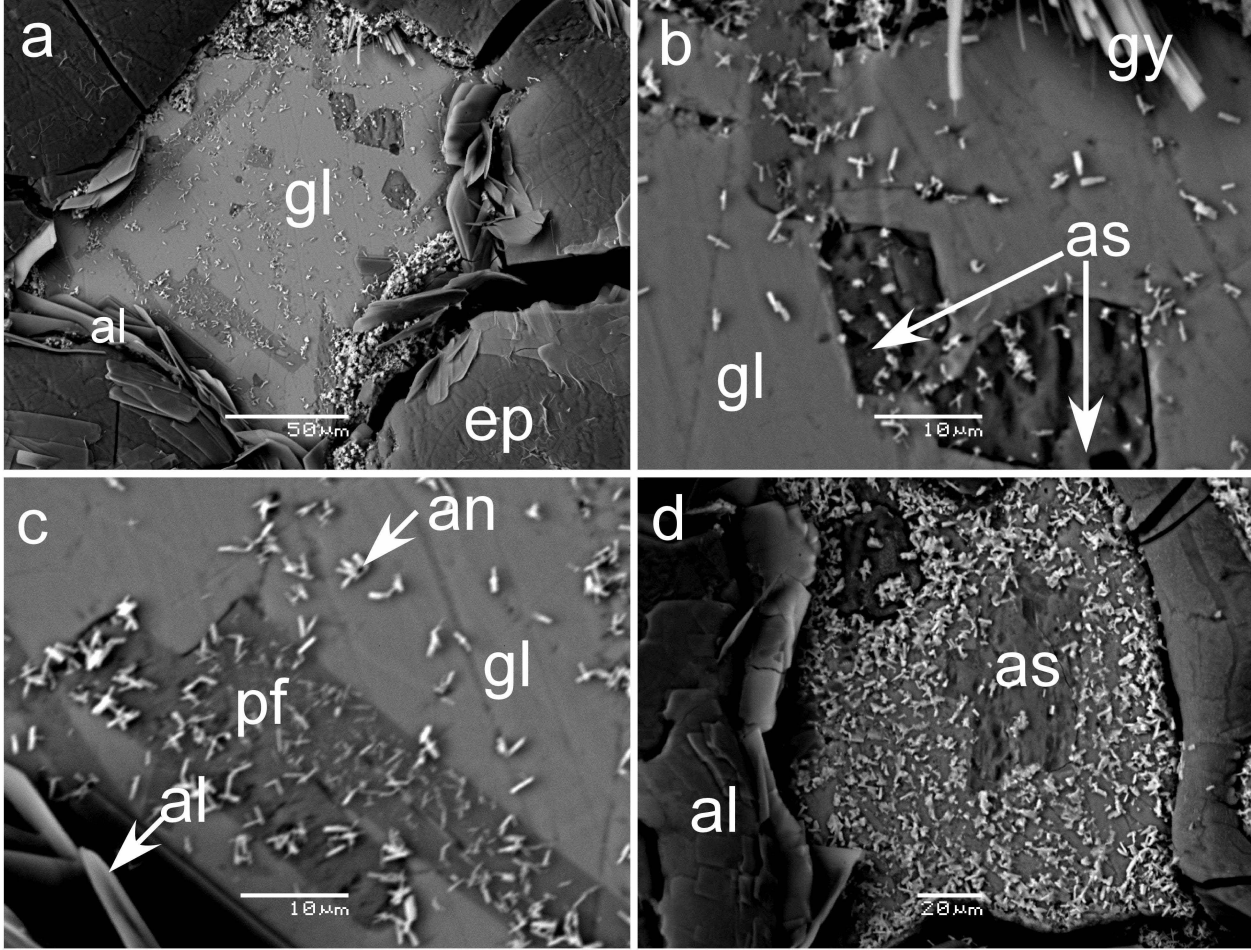
a
gl
al
50µm
ep
b
gy
as
gl
10µm
c
an
gl
pf
al
10µm
d
as
al
20µm

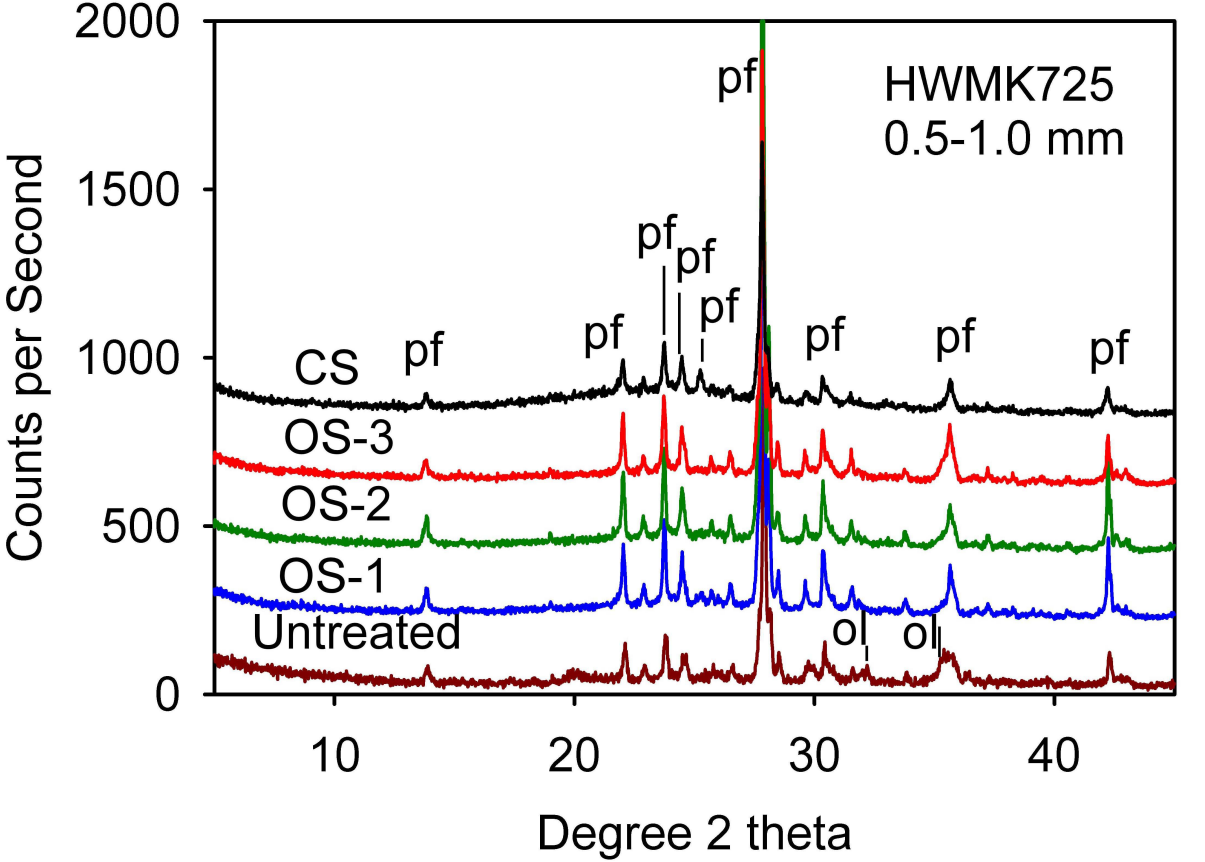
2000
1500
1000
500
0
Counts per Second
10
20
30
40
Degree 2 theta
HWMK725
0.5-1.0 mm
CS
OS-3
OS-2
OS-1
Untreated
pf
ol

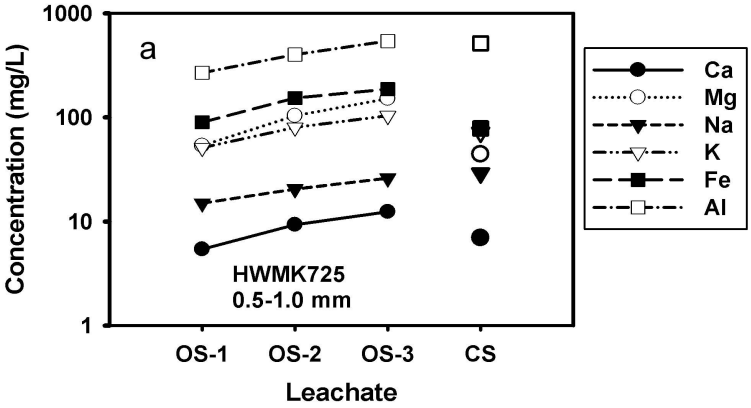
a
Concentration (mg/L)
1000
100
10
1
HWMK725
0.5-1.0 mm
OS-1
OS-2
OS-3
CS
Leachate
Ca
Mg
Na
K
Fe
Al

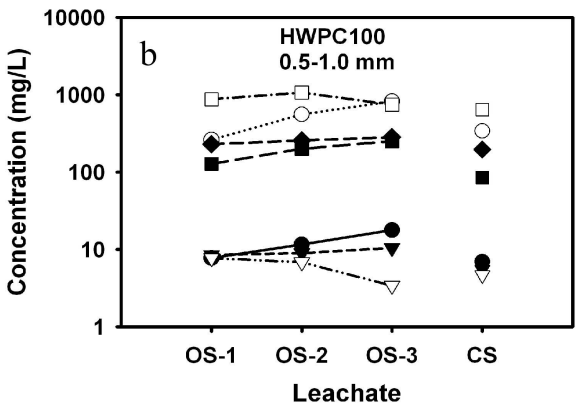
b
HWPC100
0.5-1.0 mm
Concentration (mg/L)
10000
1000
100
10
1
OS-1
OS-2
OS-3
CS
Leachate

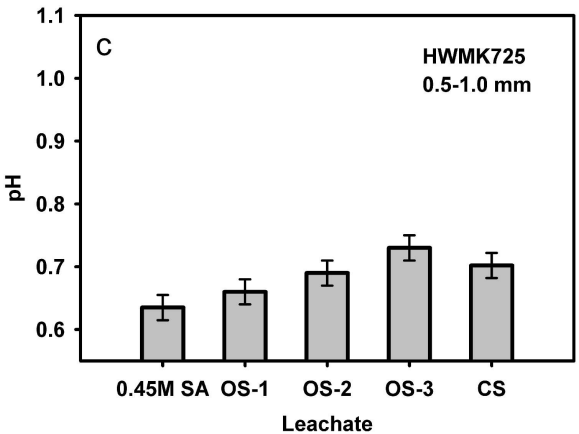
c
HWMK725
0.5-1.0 mm
pH
1.1
1.0
0.9
0.8
0.7
0.6
0.45M SA
OS-1
OS-2
OS-3
CS
Leachate

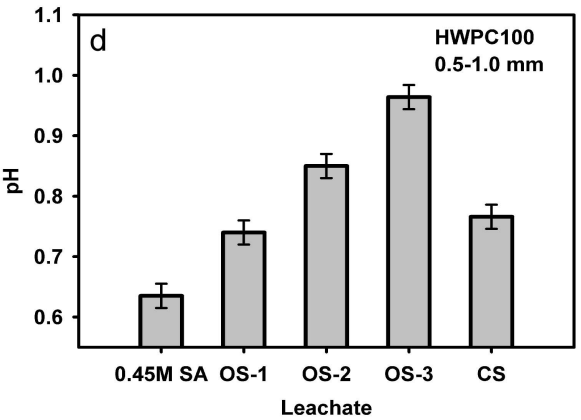
d
HWPC100
0.5-1.0 mm
pH
1.1
1.0
0.9
0.8
0.7
0.6
0.45M SA
OS-1
OS-2
OS-3
CS
Leachate